SECRET

COR-1322
Copy 2 of 5
6 September 1961

MEMORANDUM FOR: Chief National Photographic Intelligence Center

THROUGH : Acting Chief, DPD-DD/P

SUBJECT : ITEK Final Report of Frequency Attenuating Filters for Image Enhancement.

1. Attached for your information and file are five (5) copies of Contractor's Final Report covering the design and construction of subject filters.

2. This report constitutes Contractor's completion of Task Order No. 1 under the contract. Accordingly, your comments and/or approval are requested in order that final payment can be made. Further, instructions are requested regarding disposition of the Image Enhancement Viewer loaned to ITEK for their studies.

SIGNED

25X1A [redacted]

Contracting Officer

Attachments:
5 cy's COR-1306

25X1A CS/DPD-DD/[redacted]
Distribution:
1-NPIC w/5 cy's COR-1306
1-CS/DPD-BB-425 w/1 cy COR-1306
1-FIN/DPD
1-A/CH/DPD
1-RI/DPD

DOCUMENT NO. 25
NO CHANGE IN CLASS. ☒
☐ DECLASSIFIED
CLASS. CHANGED TO: TS S C
NEXT REVIEW DATE: 2011
AUTH: HR 70-2
DATE: 9 July 81 REVIEWER: 008632

SECRET

SPECIAL HANDLING

COR-1306
COPY 1 OF 2

SHC61-9019-228

Copy # 1

August 25, 1961

Dear Jim:

Enclosed please find six (6) copies each of the final report to Task Order No. 1 to Contract BB-425, entitled Design and Construction of Frequency Attenuating Filters, dated 15 August 1961.

Very truly yours,

STATINTL

Contracts Manager

HAM:pjf

Enclosures (6)

SPECIAL HANDLING

Encl #1
COR-1306
COPY 1 OF 6
IL 9019-1

DESIGN AND CONSTRUCTION of FREQUENCY ATTENUATING FILTERS

FINAL REPORT

15 August 1961

STATINTL

Prepared by:

STATINTL

Approved by:

Manager, Optics Department
Graphic Information Research Division

Itek Laboratories
Lexington 73, Massachusetts

CONTENTS

FIGURES

TABLES

1. INTRODUCTION

1.1 PURPOSE AND SCOPE OF THE PROGRAM

The aim of these project studies has been to investigate the feasibility of frequency attenuating spatial filters and, should their use prove feasible, to devise a practical method for constructing such filters. It is known that the filters presently installed in the Image Enhancement Viewer (sharp cutoff, occluding filters) do not truly enhance images, but operate on their diffraction patterns in a manner which removes image tone, raises the contrast about an edge, and gives evidence of its use by leaving ghost images or frequency "ringing". Preliminary theoretical studies have pointed out that attenuating spatial frequencies (rather than eliminating them) should not only preserve image tone, but also provide true enhancement. Such a filtering method, frequency attenuation, would obviously be useful for improving the fine detail of aerial photographs. Here the natural degradation of sharp images which results from the optical and photographic process could be compensated for. The acutance could be improved: details which were normally just below the visual threshold could be rendered visible.

The contract was undertaken to consider the following specific areas of study and development:

1. Extend previous theoretical studies on frequency attenuating filters to ascertain feasibility, and apply these results to the design and construction of such filters.
2. Develop a method for constructing frequency attenuating filters, build or purchase necessary equipment and establish specifications on materials for making such filters.
3. Construct a set of filters (should feasibility be demonstrated) which could be installed in the Image Enhancement Viewer. The maximum number of such a set was specified at four.
4. Report the results and evaluate the enhancement produced by such filters, quantitatively if possible. Such a report would present specific recommendations for extending the work.

Many facets of study are possible in such a research program. To concentrate efforts on feasibility determination and filter fabrication, several restrictions were placed on the program immediately. It was recognized early in the program that there were three basic methods of producing continuous attenuation (variable transmission) having rotational symmetry.* These were 1) mechanical, 2) evaporation of suitable materials in vacuum and 3) photographic.

---

*This is a basic requirement for non-specialized spatial filters, and is discussed in detail in a subsequent section.

The detailed development of the first method would not have allowed time to understand the basic problems in frequency attenuation. The second method required equipment and techniques beyond the (then) present capabilities of these laboratories. The third method not only did not require more than present state-of-the-art developments, but the basic techniques could be applied to the ultimate solution of the first two. Further, more time and effort could be spent in developing the underlying concepts of frequency attenuating filters. Therefore, at the onset of the program, all filter fabrication was restricted to the photographic method.

The second restriction came as a result of the theoretical investigations. A pulse or edge model was a basic theoretical requirement, and must necessarily reflect the actual, physical fact. Once established, standard analytical techniques could be applied to ascertain the type of filter to best enhance this model.

In view of the difficulty of finding a suitable model (it was not until well along in the study program that such a model was devised), the optimum filter for edge enhancement was not established. In choosing a filter shape which past experience had indicated would probably work, efforts were spent in constructing a set of filters based on an assumed rather than a derived shape. As the theoretical and experimental developments will show, this filter does enhance. What has not been established as yet is if it is the best filter for the job. This remains to be investigated.

Then, within these two basic restrictions, the research was carried out as planned. Several necessary items of equipment were designed and constructed, and the spatial filters produced. Tests indicate feasibility, within certain very specific limitations, all related to the glass filter material. These are covered in the discussions and conclusions of Section 5.

1.2 SUMMARY OF THIS REPORT

This report covers the details and results of the work carried out in performance of the contract for investigating frequency attenuating filters. The first section summarizes the theoretical results. It mathematically describes frequency attenuating filters of a specific kind (Gaussian), and predicts their effect on a spatial pulse for which a special model has been developed. The sections following cover the mechanical and sensitometric bases for filter fabrication and describe how the spatial filters are made. A section is then discussed which reports tests on the filter material and evaluates the results of filtering a typical aerial photograph.

Finally, the results are evaluated in light of the contractual requirements, and some conclusions reached. Recommendations are made, as a result of these conclusions, for the continued development of the Image Enhancement Viewer.

2. SUMMARY OF THEORETICAL INVESTIGATIONS

2.1 INTRODUCTORY CONSIDERATIONS

For the development of spatial frequency attenuating filters, several theoretical problems must first be considered. From these analyses will come the required filter shape, performance and parametric optimization.

Recently completed research,[1] using a sharp spatial pulse, dealt with filter evaluation. Enhancement, or image improvement, was not considered since little could be done to improve, per se, a sharp pulse which had a contrast of unity and an infinite slope on the edge. The first problem of the current research program was to develop a pulse model which would analytically show improvement. A pulse was considered for analytical purposes because of its symmetry, but the results would be applied to edges (which are simply one-sided pulses). The pulse concept is a simplification of what actually occurs in the rendering of fine detail in a photographic transparency. Analytically, a pulse and its edges should respond the same physically provided the model is verisimilar. The development of such a non-sharp pulse model will be facilitated by a brief discussion of the photographic edge where the abstract edge concepts can be more definitely characterized.

2.2 THE PHOTOGRAPHIC EDGE

A photographic edge represents, in a general sense, the boundary between contiguous regions of differing densities. There are two important variables which control this boundary: 1) the macroscopic density difference between the contiguous regions, and 2) the size of the microscopic region or zone of transition from one density to the other. Density difference affects the ability of a human observer or densitometer comparator to discover the existence of an edge, since there is a difference impossible to detect. This difference will vary for the mode of observation, but such a threshold does exist. It establishes the basic energy limitation for subsequent photographic processes or intensifiers to delineate the edge by amplification of the difference across it.

The size of the transition zone is more immediately useful, since it not only provides a convenient basis for differentiating between sharp and non-sharp edges, but will also aid in determining the general characteristics of edge or pulse models. If the microscopic area of the photographic emulsion which bridges the gap between two differing densities is called the zone of transition, the following definitions can be made: when the change of density across the zone of transition is spatially instantaneous, the edge is said to be sharp; when the change is gradual and continuous, the edge is said to be non-sharp. The size of the zone is therefore a good measure of edge non-sharpness and gives an indication of the degrading effect of the antecedent optical and photographic processes.

In general, a quality which describes the variation of density across this zone is "smoothness" or lack of definition. The end points are ill-defined, and the transition is continuous. Thus, any edge or pulse model should have this smooth, continuous characteristic, allow for

adjustment to various zone sizes, and reduce to a sharp edge or pulse in the limiting case. It should be kept in mind that such a simplification could not possibly represent an edge modified by the Eberhardt effect. Such non-linear variations cannot be handled by simple models.

2.3 NON-SHARP, GAUSSIAN PULSE MODEL

The several criteria deduced in the foregoing discussion of photographic edges can lead to more than one pulse model, but none through an appeal to first principles. The Gaussian form has found usefulness in several instances[2,3], and appears to be a reasonable fit to a wide range of photographic edge phenomena. Figure 1 is the microdensitometer trace* of a photographic edge obtained by photographing a sharp edge with a pinhole camera. This has been fitted with a Gaussian, shown by the dashed line. The agreement is very good for edges of this type.

A Gaussian pulse may be written, generally, as

$$f(x) = T_1 + (T_2 - T_1)\, e^{-c\,x^2}, \tag{1a}$$

or

$$f(x) = T_2 - (T_2 - T_1)\, e^{-c\,x^2}, \tag{1b}$$

depending on whether the pulse is centered about a low or high transmission value. The edge of Figure 1 is of the form of equation (1a). For these equations,

T_1 = minimum transmission value

T_2 = maximum transmission value

c = pulse rise (or drop-off) coefficient

x = object coordinate

This function satisfies the edge criteria analytically, and has the necessary degrees of freedom to be fitted to a wide variety of edges. Figure 2 is a plot of equation (1a), using arbitrary transmission values.

Under the assumption that such a pulse resulted from the degredation of a sharp pulse, the purpose of enhancement is to reconstruct (as best possible) the original pulse shape from the information contained in the degraded, non-sharp pulse.

One of the important constants of this equation is the variance, or abscissa corresponding to the half-power point, a measure of pulse width. This is useful not only in empirically fitting edges to the assumed Gaussian form, but also, as will be shown later, in determining the size of the optimum Gaussian attenuating filter. This quantity is obtained by doubly differentiating equation (1a) or (1b), equating the result to zero, and solving for $\underline{x}$. This produces,

$$x = \pm \frac{1}{\sqrt{2c}} \tag{2}$$

Before considering the imaging of such an object pulse, a discussion of attenuating filters would seem to be in order. However, it will be restricted to the type considered in these investigations.

---

*The ordinate of this and subsequent traces may be converted to optical density through Figure 14.

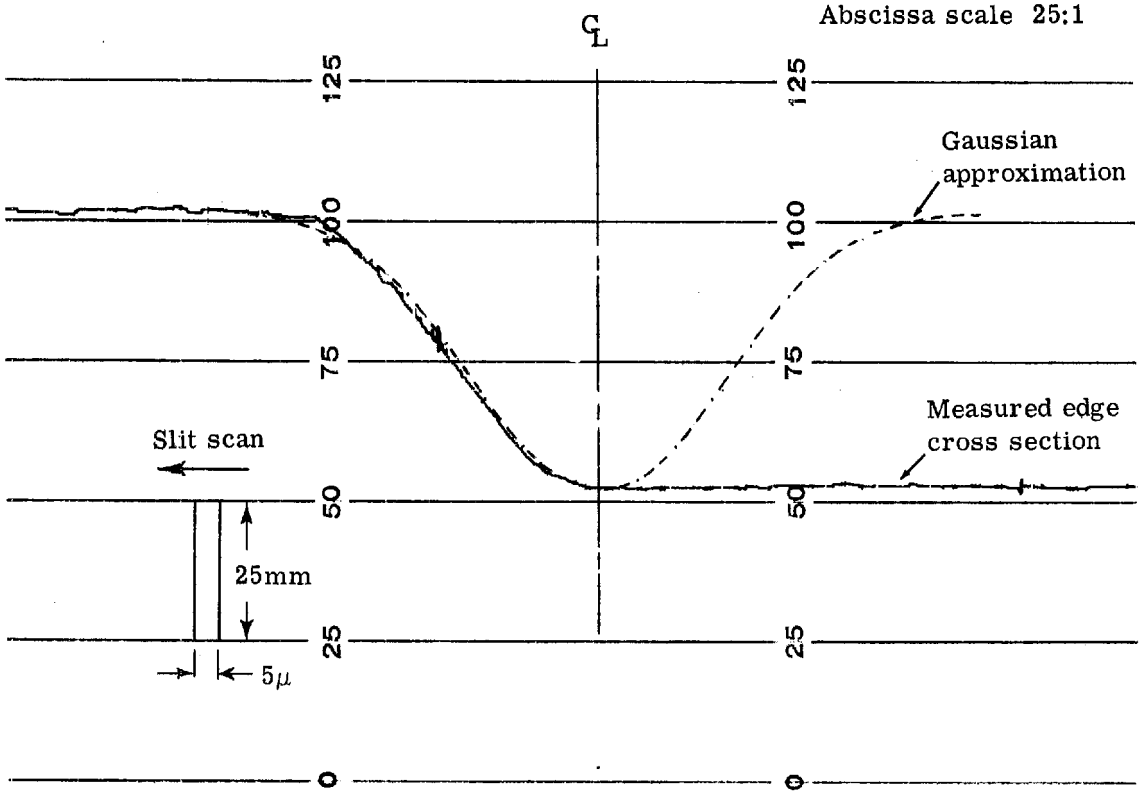

Fig. 1 — Experimental edge trace approximated by a Gaussian (portion of Gaussian to right of centerline is shown only to establish the shape more clearly)

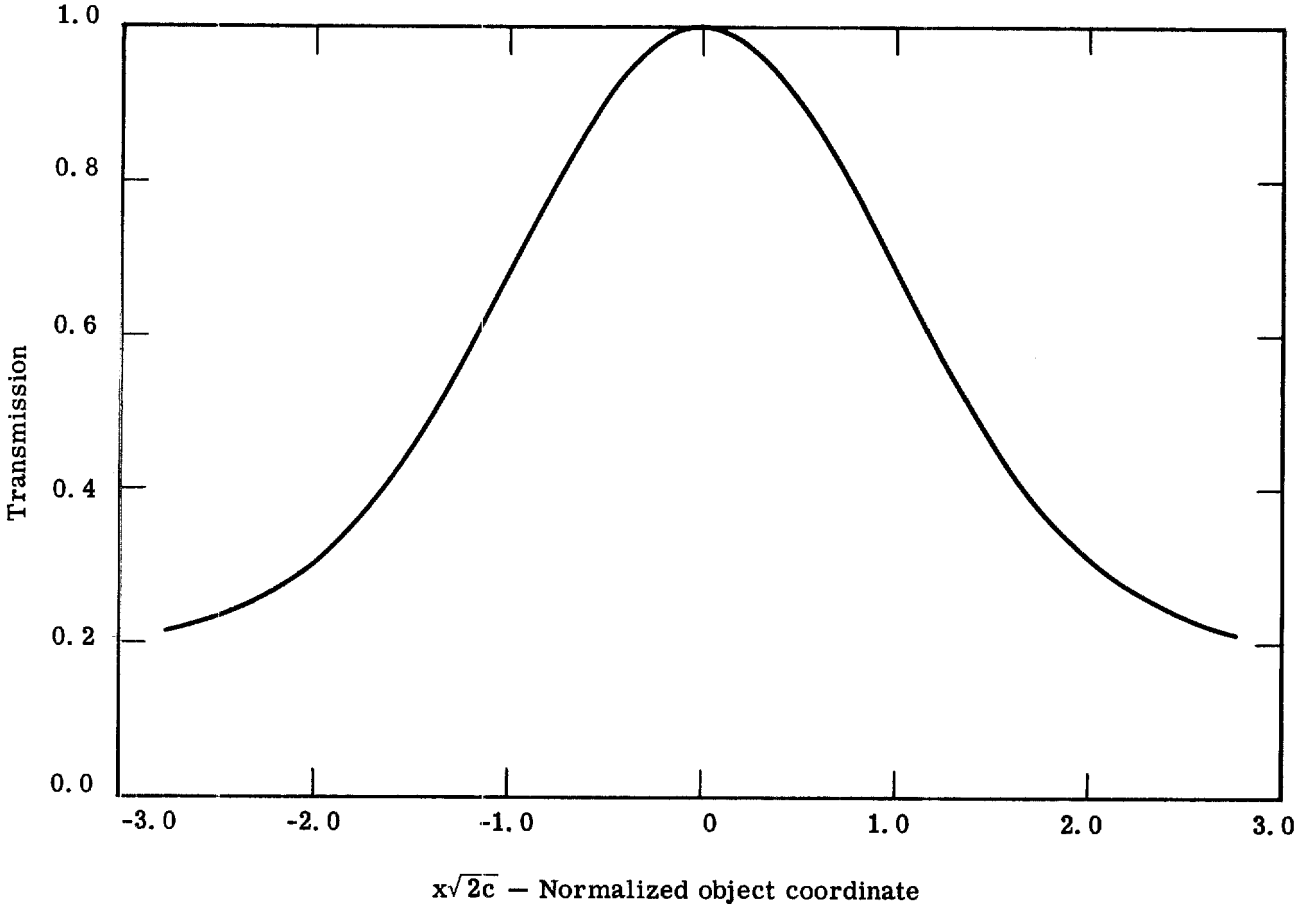

Fig. 2 — Typical Gaussian spatial pulse

2.4 FREQUENCY ATTENUATING, GAUSSIAN FILTERS

In view of the lack of theoretical basis for determining the "optimum" attenuating filter, there is no preferred filter shape. However, past experience has shown that there are two important considerations which can provide some insight into the problem:

1. Low-pass filtering will not enhance or improve edges, since it removes the requisite high spatial frequencies.
2. An occulding filter will "ring", and, in blocking out the center of the diffraction pattern, will remove the basis of image tone.

From these it may be concluded that any shape chosen for attenuating filters should be high-pass, while the transmission in the center should not be low enough to occlude.

Such a filter shape, of continuous density variation, is exemplified by a Gaussian which is dark in the center and changes smoothly to high transmission at the edges.* It can be shown that the one-dimensional analytical form of such a filter is written

$$G(w) = \frac{T_2 - T_1 e^{-\beta w^2 f}}{1 - e^{-\beta w_f^2}} - \frac{(T_2 - T_1) e^{-\beta w^2}}{1 - e^{-\beta w_f^2}} \qquad (3)$$

where

w_f = upper cutoff frequency due to the field stop in the diffraction plane, and

β = filter-rise (or drop-off) coefficient, similar to the $\underline{c}$ for the pulse in equation (1).

Considering filters whose variance is small compared to the extent of frequency space, i.e.,

$$\beta >> \frac{1}{w_f^2}, \qquad (4)$$

equation (3) may be simplified to

$$G(w) = T_2 - (T_2 - T_1) e^{-\beta w^2}, \qquad (5)$$

and is identical in form to equation (1b).

---

*The following filter shape, based on the preceding criteria was also studied:

$$f(w) = T_1 + (T_2 - T_1) [w - \frac{1}{2\pi} \sin (2\pi w)]^2.$$

It was found to possess sufficient "fitting" properties to cover several edge types. This shape is sufficiently general to be used as a spatial pulse, in a manner analogous to equations (1a) and (1b). Such a pulse and filter were studied, but the mathematical tractability was low and they were discarded in favor of the Gaussian forms.

For purposes of demonstrating the one-dimensional shape of such a filter, equation (5) is plotted in Figure 3. T_2 is assumed equal to unity, and T_1 is varied as a parameter. The obvious effect is to achieve an "inverted" spatial pulse, but its use in the plane of diffraction changes both its analytical meaning and physical manifestation. Consider, next, the image of a pulse passed through such a filter.

2.5 IMAGE OF A GAUSSIAN PULSE THROUGH A GAUSSIAN FILTER

Following the systematic analysis described and utilized in OD-61-6[1], the spectrum of a Gaussian pulse in a linear, coherent optical system may be written

$$F(w) = T_1 \int_{-\infty}^{\infty} e^{-iwx}\, dx + (T_2 - T_1) \int_{-\infty}^{\infty} e^{-cx^2} e^{-iwx}\, dx, \tag{6}$$

using equation (1a) for the pulse-form, and considering the pulse in one dimension only.

Under the assumption that the pulse width is small compared to the field stop, x_f, in object space, or

$$c >> \frac{1}{x_f^2},$$

equation (6) becomes

$$F(w) = 2(x_f)\,(T_1)\,\mathrm{sinc}\,(wx_f) + (T_2 - T_1)\sqrt{\frac{\pi}{c}} \cdot e^{-w^2/4c} \tag{7}$$

$$= \text{Field Stop spectrum} + \text{Pulse spectrum.}$$

As in OD-61-6, the field stop spectrum can be eliminated analytically since it contributes only a bias or base energy term (whose significant contributions occur in the vicinity of the origin). Subsequent analytical considerations need account for this missing term only for purposes of interpretation of results.

Basing further considerations on the pulse spectrum alone, the image is given by its Fourier Transform, and following OD-61-6, the image is written

$$h(z) = \frac{(T_2 - T_1)}{2\sqrt{\pi c}} \int_{-\infty}^{\infty} G(w)\, e^{-w^2/4c}\, e^{iwz}\, dw, \tag{8}$$

where G(w) is the spatial filter.

Passing the pulse through a Gaussian filter is equivalent to evaluating equation (8) using equation (5) as G(w). Then

$$\frac{h(z)}{P(T_2 - T_1)} = \frac{f_{T_2}}{\sqrt{\pi c}} \int_{-\infty}^{\infty} e^{-w^2/4c} \cos(wz)\, dw$$

$$- \frac{f(T_2 - T_1)}{\sqrt{\pi c}} \int_{-\infty}^{\infty} e^{-\left(\beta + \frac{1}{4c}\right)w^2} \cos(wz)\, dw. \tag{9}$$

under the assumption that pulse and filter widths are small enough, compared with their respective field stops, to extend the limits of integration to infinity.* Equation (9) can be evaluated immediately, in closed form and the image of a Gaussian pulse passed through a high-pass Gaussian filter is given by

$$\frac{h(z)}{p(T_2 - T_1)} = {}^{f}T_2 e^{-cz^2} - \frac{{}^{f}(T_2 - T_1)\, e^{-\left(\frac{cz^2}{4\beta c+1}\right)}}{\sqrt{4\beta c + 1}} \qquad (10)$$

The first term on the right-hand side can be recognized as the image of the object pulse, without the bias term. Then the image shape will differ from the object shape according to the magnitudes of $4\beta c$ and ${}^{f}(T_2 - T_1)$. The observable quantity is intensity. Therefore, before treating the various filtering possibilities it will be necessary to square equation (10), an amplitude distribution, to obtain the analytical form of intensity.

In Figure 4, image intensity is plotted against a normalized image coordinate for several values of the $4\beta c$ product, at a constant T_2 and T_1. The ordinate normalizations were obtained by requiring the areas under the curves to be equal. The curves of Figure 4 demonstrate a definite improvement in image edge gradient and contrast when the pulse is passed through a Gaussian filter.† The pulse has been narrowed and steepened, although some low-intensity ringing has occurred. Thus, for the assumed pulse model and frequency attenuating filter combination, it appears possible to materially increase the edge gradient without destroying image tone and adding large amounts of "ringing" or edge fringing.

The next logical problem is the optimization of the filter constants for specific enhancement criteria. Such a consideration will determine the basis for selection of practical filters for the image Enhancement Viewer.

2.6 OPTIMIZING GAUSSIAN FILTER CONSTANT

Since the filter variance, β, and the pulse variance, c, are multiplicatively related, a given filter will affect pulses whose variances fall within the useful range of the $4\beta c$ product. This would indicate that there is no optimum, as far as β is concerned, unless it be for a specific pulse. The choice of β's is therefore predicated on the gradients of pulse edges to be encountered in practice. However, by choice of a suitable criterion, it may be possible to utilize the ${}^{f}(T_2 - T_1)$ quantity for optimizing some image feature.

Figure 4 indicates that a useful basis might be the minimizing of the first zero of the filtered image intensity. This would have the advantage of steepening the pulse edge and raising the height of the pulse center. It is equivalent, in effect, to maximizing the acutance. There are other possible criteria, particularly the maximizing of the slope of the image intensity, at, for example, the inflection point. However, this would be the result of minimizing the abscissa of the first image intensity zero, as already proposed. The first choice, then, is not as arbitrary as it might first have appeared.

The basic problem consists in first solving equation (10) for z, when h(z) goes to zero. Then two partial derivatives of z are taken separately: the first with respect to $4\beta c$, the second with respect to ${}^{f}(T_2 - T_1)$. These two equations are then set equal to zero and solved simultaneously for $4\beta c$ and ${}^{f}(T_2 - T_1)$. The solutions constitute the optimum values for the specified criterion.

---

* The superscripts p and f denote the transmission values of pulse and filter, respectively.
† An alternate way to note this enhancement is to state that the acutance has been improved.

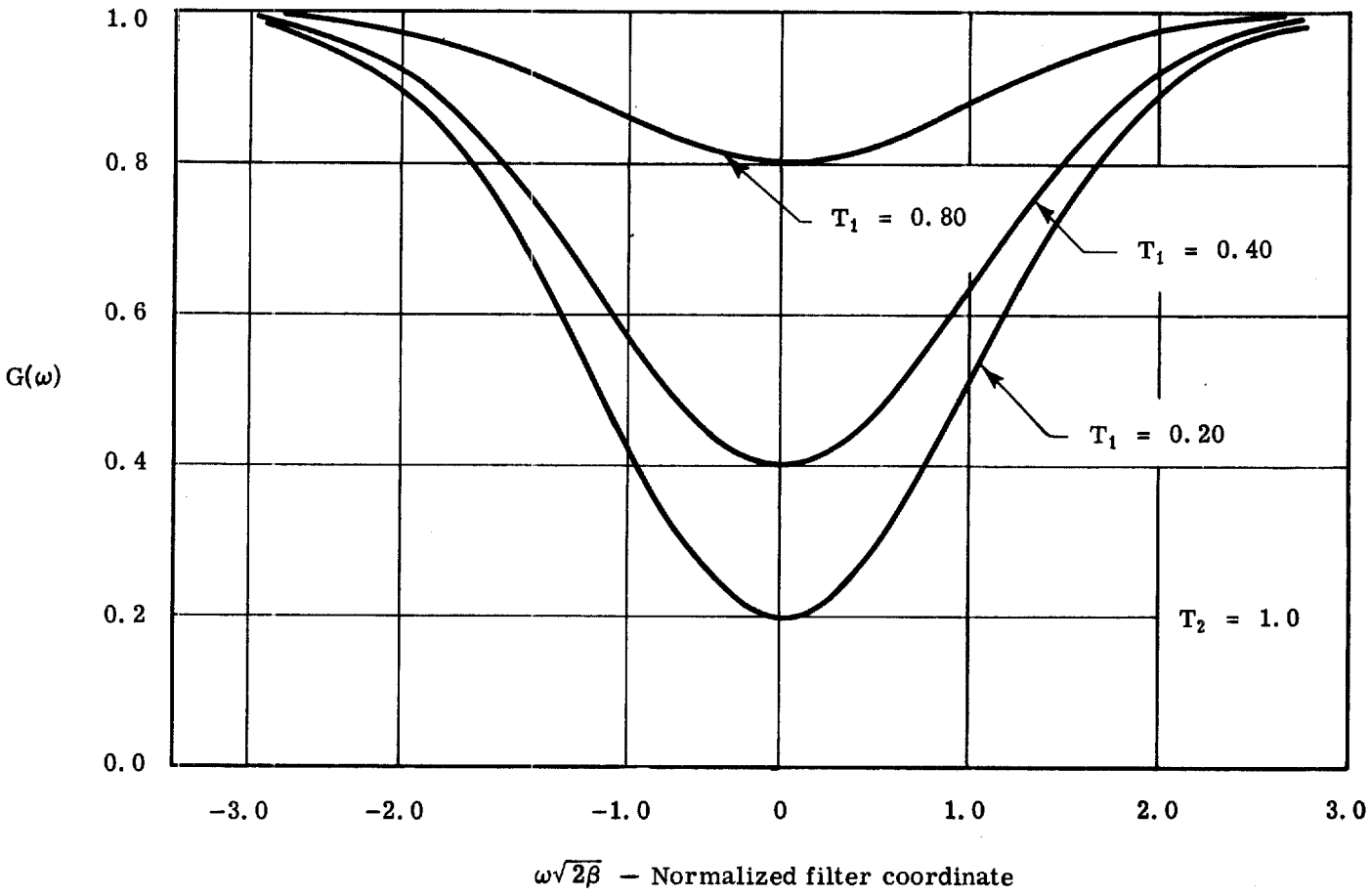

Fig. 3 — Plots of typical Gaussian high-pass filters, showing the variation due to the central transmission value

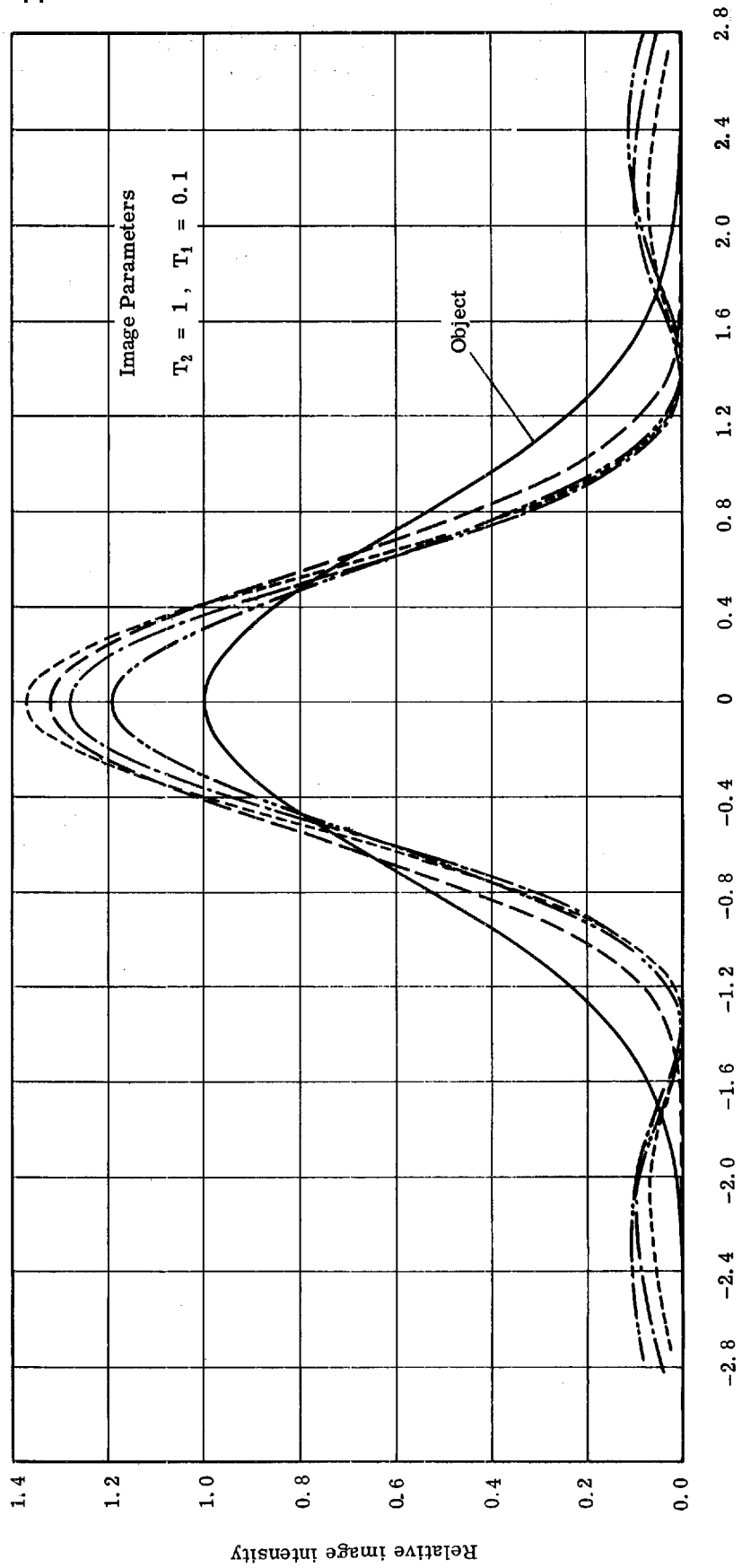

Fig. 4 — Image intensity of a Gaussian pulse passed through a high-pass Gaussian filter, showing the parametric variation due to the $4\beta c$ term

Actually, the second of these equations vanishes identically, indicating a functional dependence of $4\beta c$ and $f(T_2 - T_1)$. It can be shown that these quantities are related by the equation

$$\frac{T_1}{T_2} = 1 - (\sqrt{4\beta c + 1})\, e^{-2\beta c}. \tag{11}$$

The principal usefulness of this equation is to provide a transmission ratio (once a $4\beta c$ product has been chosen) which places the first zero of the image intensity closest to the origin, and maximizes the acutance. The relationship will be used later to determine the actual working filter constants.

2.7 ADDITIONAL THEORETICAL CONSIDERATIONS

There are several analytical problems that were not considered in these investigations, primarily because they depended on a suitable pulse model which was not obtained until late in the research program. Probably the most important analytical problem remaining is a study of optimum filtering. The present analysis assumes a Gaussian filter form in view of the lack of a definite theoretical basis. An analysis should be carried out through the variational calculus to determine the optimum G(w) for specific enhancement effects. Now that a suitable pulse model has been established, the problem should involve only the application of known analytical techniques. A simultaneous study to devise a means of analytically assessing the enhancement effects of attenuating filters would also be of great value.

2.8 SUMMARY

A theoretical pulse model has been devised and an analysis made of its imaging through a linear, coherent optical system, using a spatial filter of Gaussian cross-section. The analysis indicates that such a shape provides a definite enhancement, and establishes a relationship between the significant parameters for optimum enhancement. Specific areas for future study are indicated and their usefulness briefly discussed.

3. SPATIAL FILTER FABRICATION

3.1 MECHANICAL BASIS

3.1.1 Requirements

The general spatial filter shape characteristics to be considered in these investigations may be listed as follows:

1. Rotational symmetry about the optical center
2. Continuously varying attenuation (without discontinuities)
3. Non-occluding.

The first consideration is due to the fact that while diffraction patterns of photographic transparencies which contain images of man-made objects generally have a preferred orientation, the frequency content is symmetric about the frequency axes. When the filter is rotationally symmetric, it allows for arbitrary planar orientation of the object transparency. Filters which are selective with respect to orientation generally violate the second and third shape considerations, and are designed for specific tasks beyond the scope of these investigations.

The second consideration results from a need not only to eliminate a sharp cutoff which would result in image "ringing", but also to allow the widest possible range of filter cross sections. Previous studies have shown the third consideration necessary to maintain the full image tonal range. Additionally, by making filters non-occluding, more energy (on the average) should be available for the formation of the aerial image.

3.1.2 Basic Manufacturing Technique

In view of the requirements for rotational symmetry, it will be necessary to provide means for obtaining a given optical density, over 2π radians, at a specified radius from the filter center. This can be achieved by exposing a suitable photographic material which is rotating at a fixed speed, to a collimated beam, through an aperture whose shape is a function of the required filter cross section. A diagram showing the basic ideas is shown in Figure 5. The fixed and rotating planes are parallel to each other and perpendicular to the collimated beam. Such a scheme would be adaptable for evaporating metal or dielectric films in vacuum. The principle difference would be in the law of optical density formation.

Another variation of this basic technique would be to insert a rotating aperture directly in the plane of diffraction and allow the resulting attenuation to produce the filtering, on an integrating basis. This method would require extensive mechanical modification of the Image Enhancement Viewer. It would tend to add vibrations which could degrade image quality. Finally, it would require dynamic alignment and continual stabilizing readjustment* as parts respond to

* This is done so that in rotating, the center portion would not block out, or occlude the diffraction pattern center which would destroy image tone.

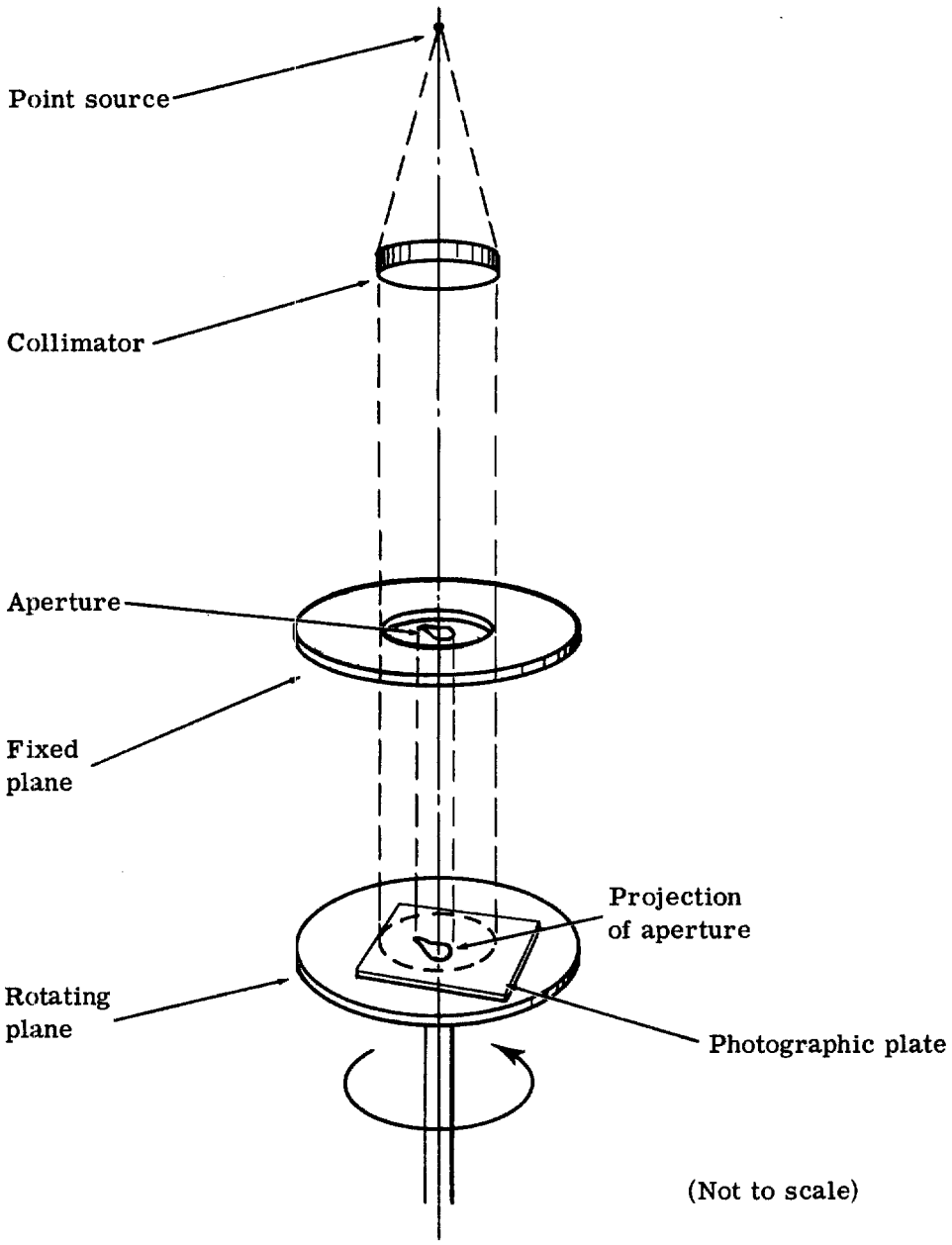

Fig. 5 — Diagram showing basic concept for achieving rotationally symmetric photographic exposure

temperature variations and frictional wear. Such a method would have the singular advantage of no glass (which could introduce wedge or add phase errors to the wavefront) in the optical system.

The rotating plate method was chosen as the basis for filter fabrication because it was relatively simple to realize practically, and because the results obtained through photographics would apply (with some modification) to vacuum deposition and mechanical methods. It was realized that commercially available photographic plates (even on special order) were not suitable for maintaining flat-frequency response over the system passband. It was felt, however, that through their use the feasibility of such filtering could be established and specifications determined.

3.1.3 Aperture Shape

A method for determining aperture shape must first be established before designing and constructing an exposure device. It will be sufficient to establish a mathematical relationship between the required filter cross-section and exposing aperture shape. This can be carried out in a polar coordinate system, which will specify a radius and an angle for each point on the aperture contour.

The finished filter will constitute a distribution of optical density (or transmission), with circular symmetry, on a photographic plate. This distribution will be denoted $T(\bar{r})$, where the bar signifies a radial coordinate normalized to the maximum field stop:

$$\bar{r} = \frac{r}{r_{max}} \quad . \tag{12}$$

Some exposure produced $T(\bar{r})$, and it may be described functionally as

$$T(\bar{r}) = f\ [E(\bar{r})] \ . \tag{13}$$

Now exposure (in the absence of reciprocity failure, intermittency, and other mitigating effects) can be written for the scheme of Figure 5,

$$E(\bar{r}) = (I_o t)\ w \frac{s(\bar{r})}{\bar{r}} \ , \tag{14}$$

where

I_o = illumination intensity

t = exposure time

w = rotational speed of turntable (RPM)

$s(\bar{r})$ = arc length of aperture opening, at some $\bar{r}$

$\bar{r}$ = normalized radius to some point on aperture

Since

$$\frac{s(\bar{r})}{\bar{r}} = \Theta\ (\bar{r}) \ , \tag{15}$$

and because $(I_o t)\ w$ is constant for a given exposure, equation (14) may be simplified.

$$E(\bar{r}) = C\ \Theta\ (\bar{r}) \ , \tag{16}$$

where

$C = (I_o t)w$ = constant = base exposure.

$\Theta(\bar{r})$ = Angular separation of mask opening at a given radius, $\bar{r}$.

The $E(\bar{r})$ of equation (16) is that produced by the exposure device. The f $[E(\bar{r})]$of equation (13) is that required to produce the filter. Hence the two exposures must be equal. The latter may be written inversely as

$$E(\bar{r}) = g\,[\,T(\bar{r})]\ . \tag{17}$$

Such an inversion may be accomplished by a reversion of series [assuming $T(\bar{r})$ can be expanded as a power series in $E(\bar{r})$], or by graphical means. Then equating the exposures of equations (16) and (17),

$$g\,[T(\bar{r})] = C\,\Theta(\bar{r}) \tag{18a}$$

or

$$g'\,[\,D(\bar{r})] = C\,\Theta(\bar{r})\ , \tag{18b}$$

the latter considering density as a result of $E(\bar{r})$. Equation (18b) is probably more useful since sensitometric results are generally displayed as a plot of Density versus a function of Exposure.

For a high-pass filter, $D(\bar{r})$ is a maximum at the center, where $\bar{r} = 0$. The $\Theta(\bar{r})$ should also be a maximum there. The constant, C, is thereby determined,

$$C = \frac{g'\,[D(0)]}{\Theta(\bar{r})_{max}} = \frac{E(\bar{r})_{max}}{\Theta(\bar{r})_{max}}\ , \tag{19}$$

holding the exposure illumination, time, and rotational speed fixed. Combining this with equation (18b), gives the required relationship for high-pass filters,

$$\Theta(\bar{r}) = \frac{\Theta(\bar{r})_{max}}{g'[\,D(0)]} \left\{ g'\,[\,D(\bar{r})]\right\}, \tag{20a}$$

or

$$\Theta(\bar{r}) = \frac{\Theta(\bar{r})_{max}}{E(\bar{r})_{max}} \left\{ E(\bar{r})\right\}. \tag{20b}$$

This is the equation which determines the size of the aperture, or exposure mask, given as the angular separation of each side of the opening in the mask as a function of radius. This mask must now be incorporated in a device which can use its properties.

3.1.4 Exposure Jig

A device which embodies the principles sketched in Figure 5 was designed and constructed. Photographs of this device are shown in Figures 6 and 7.

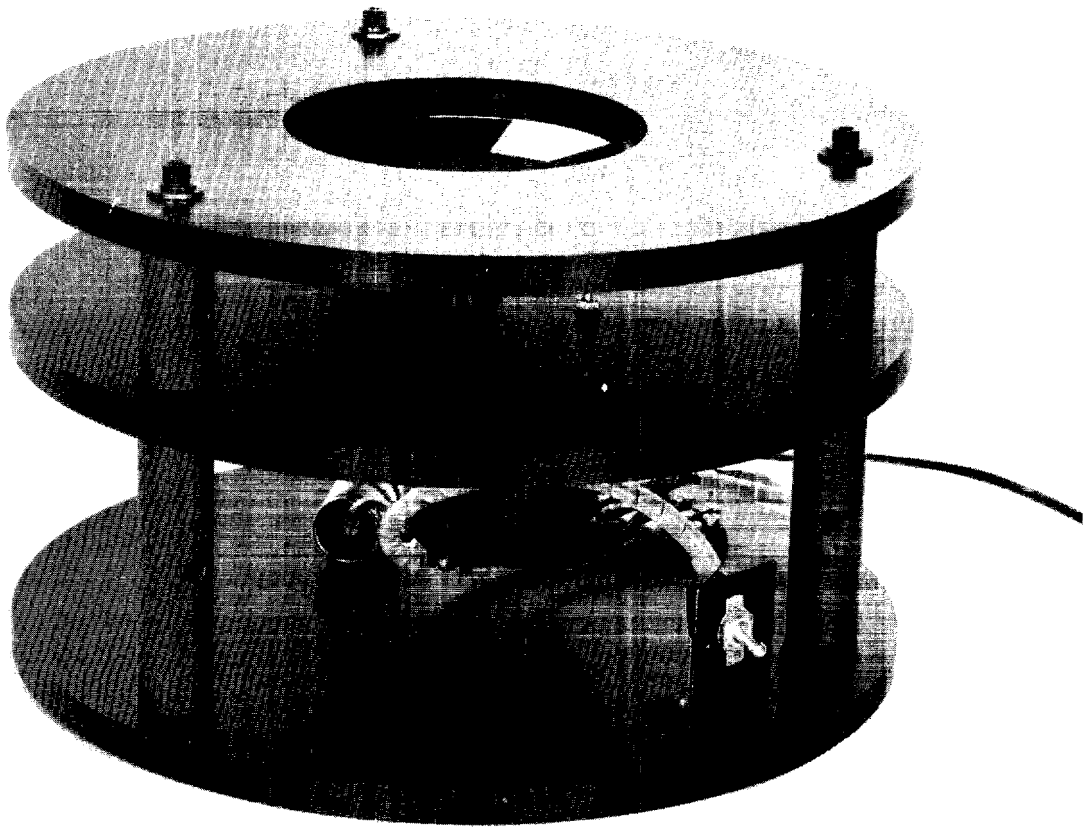

1812

Fig. 6 — View of the Exposure Jig, exhibiting the cutout in the turntable, and showing the counterbore in the center of the upper plate which holds the exposure mask

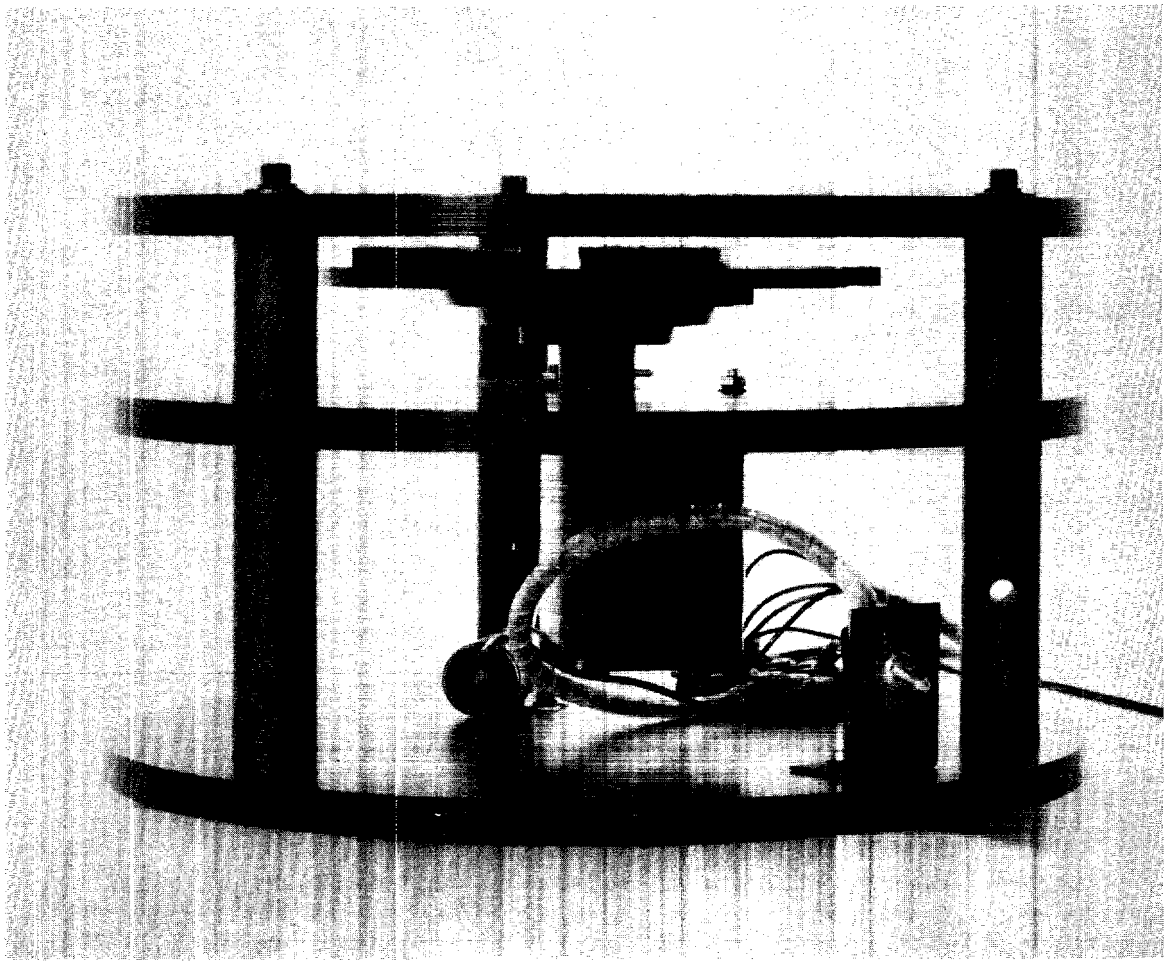

1809

Fig. 7 — View of the Exposure Jig, exhibiting the turntable details

A Borg No. 1007-4SY Synchronous motor rotates a turntable at 30 RPM, to which the photographic plate is fastened. The three parallel plates which constitute the three decks of the device are 12 ½ inches in diameter, and the unit stands 7 ½ inches high. The upper plate, the fixed plane of the exposure mask, must be centered exactly over the center of rotation of the turntable. This was positioned in a Jig-Borer and the plate locked down tightly. In order to minimize the effects due to imperfect light collimations (which would cause the illumination to diverge and require impossibly precise placement of the jig), the rotating and fixed planes were placed as close together as possible. The closeness was consistent with the capability of the human hand(s) to fit between the two top circular plates and secure the photographic plate on the turntable. A cutout on the turntable was provided to aid in inserting and removing the plate. This cutout is clearly shown in Figure 6, through the counterbored opening in the top plate.

The illumination was obtained from an incandescent lamp (GE No. 1238) placed approximately eight (8) feet above the exposure jig, and collimated through an f/8 achromatic doublet of 24.5 inch focal length. While a point source at 8 feet would have served the same purpose, the collimator provides more light intensity per unit area on the exposure mask and relieves the critical optical axis alignment problem.

In operation, the photographic plate is placed on the turntable and held in place by two gibs and a locking nut. The appropriate exposure mask is placed in the counterbored opening in the upper plate. The turntable is then set in rotation by throwing the switch located on the lower plate of the jig. A gentle stream of air is continuously played over the surface of the photographic plate to remove dirt and dust particles which tend to settle during long exposures. Finally, metered voltage is applied to the source lamp for a specified time. This is accomplished through a Gra-Lab Darkroom timer which shuts off the lamp power at the end of the predetermined exposure period. Upon stopping the turntable rotation, the plate may easily be removed for processing. The details of this processing are discussed in the next section.

3.2 SENSITOMETRIC BASIS

3.2.1 Requirements

The restriction of these filter fabrication studies to the photographic process places a premium on the selection of proper photographic materials. The following are some of the important considerations which affect this choice:

1. To accommodate a large range of filter types, the achievable density range should be large, with a very low base-density, to allow transmission approaching unity.
2. A wide range of gammas should be achievable, through the use of standard developing formulas.
3. Grain size should be small to minimize scattering effects when the developed emulsion is used as a filter.
4. To reproduce the requisite density cross sections and support them when used as filters, glass plates are necessary. Such plates provide the best dimensional stability available for photographic materials.
5. Glass plates should be as flat as possible, have minimum wedge, be strain and striae free, and be capable of being cut and edge-finished.
6. The emulsion should be as thin and uniform as possible in order not to distort the image when placed in the optical system. Hardened emulsions should not apply stress to the glass support and thereby add power to the system.
7. Glass thickness should not exceed 0.125 inch, since extensive modification of the Image Enhancement Viewer would be probable for thicknesses exceeding this.

3.2.2 Photographic Plates

Some of the requirements are mutually exclusive, and compromises therefore are necessary. After considering the available materials, Kodak High Resolution Plates were chosen for these tests. On special order, they were obtained on Ultra-flat glass which specifies flatness to within .0007 inch per linear inch. While this is not considered good optical flatness, it was the best obtainable below the specified thickness. The 0.060 inch thickness in which these plates are supplied prohibits any but minute improvements on surface flatness, since they would not be rigid enough to refigure properly.

The emulsion is exceedingly thin (virtually transparent), the maximum density and gamma very high, clear plate transmission nearly unity, and the granularity (under most processing conditions) is exceptionally small. The effect of this material in the optical system was tested thoroughly and the methods and results are reported in a subsequent section.

3.2.3 Processing

To reproduce results, a set of processing conditions were established. Developing solutions, times and temperatures, were not immediately standardized. Since development constitutes the major variational method of the process, preliminary tests were necessary to establish density and gamma characteristics.

For purposes of completeness, so that the results of this report may be reproduced by others, the standardized detailed procedure is outlined below:

1. Development: Time and Temperature as required, at constant agitation.
2. Stop Bath: 30 seconds at 65 – 72°F, with occasional agitation.
   Kodak Indicator Stop Bath solution, diluted 2 ounces per gallon of water.
3. Fix: 10 minutes, at 65 – 72°F, with occasional agitation.
   Kodak Acid Fix, full strength.
4. Wash: In running water, 30 minutes, at 65 – 72°F, with occasional agitation to remove adhering air bubbles.
5. Wash: 2 minutes in Photo-Flo solution at 65 – 72°F, with occasional agitation.
   Kodak Photo-Flo diluted 4 capfuls per gallon of water.
6. Rinse: In distilled water, until previous bath has been removed. Do not wipe or squeegee.
7. Air dry in rack.
8. Additional considerations and details:
   a. Plates are handled in Kodak Film and Plate Developing Hangers, No. 4A, 4 × 5 size. Plates are removed only for rinsing and drying of steps 6 and 7.
   b. Agitation: lift Plate hanger completely out of solution; tilt to drain, on the diagonal; replace immediately. Lift again; tilt in opposite direction; replace. This cycle should take approximately 2 seconds, and is carried out continuously througout the development.
   c. Kodak Hard Rubber Tanks are used for all processing, and filled with 62 ounces of solution. Temperature is maintained by immersing the tanks in a regulated water bath. Temperature is measured with a thermometer calibrated in degrees, which permits interpolated readings to the nearest one-half degree.

d. No more than eight 4 × 5 plates are developed in one tankful (62 ounces) of developing solution. The solution is discarded after use. The remaining processing solutions (Stop Bath, Acid Fix) are used until exhausted or until normal wastage depletes the useful supply.

3.2.4 Exposure

The plates were exposed, both for the actual filters and the preliminary sensitometric tests, in the exposure jig shown in Figure 6 and 7. The light source and collimating system have been described previously. Thus, any sensitometric testing is directly applicable to filter fabrication without reciprocity failure correction.

In order to determine the characteristics of the emulsion, so that the requirements of equation (20) could be met, two exposure masks were constructed. These masks consisted of a stepped aperture, each step varying in a prescribed fashion. One mask varied the stepped openings geometrically as 2^n, so that the ratio of the smallest to largest exposure was 128. Referred to as the Geometric Mask, it is suitable for ascertaining the sensitometric characteristics over a wide exposure range. The other mask consisted of 10 steps which varied linearly, so that the ratio of the smallest to largest exposure was 10. Referred to as the Arithmetic Mask, it is especially suited for determining the sensitometric characteristics over a short exposure range, particularly in the region of the toe. Photographs of these masks and the test plates they produce are shown in Figure 8.

3.2.5 Sensitometric Test Results

Kodak High Resolution Plates were tested for several developer types and concentrations. The results for D-76 and DK-60a are shown in Figures 9, 10, and 11, for the specific conditions shown on the plots. VHD developer was also tried, but since the film speed shifted with small processing and temperature variations, it was felt that the loss of reproducibility did not warrant further use.

Figures 10 and 11, based on the Arithmetic Mask, use a linear scale. The linearity of the toe region of the characteristic curve has been mentioned in the literature[4], and these figures corroborate such a linear trend. High-pass filters will have regions of high transmission. This places the present interest on the toe of the curve. Thus Figures 10 and 11, being more accurately defined, by virtue of the greater number of experimental points, will be used for subsequent filter manufacture. They represent the graphical form of the $g'[D(\mathbf{r})]$ or $E(\mathbf{r})$ of equation (20).

3.3 FILTER PREPARATION

3.3.1 Exposure Mask Computation and Layout

The diameter of the counterbore in the top-most plate of the exposure jig has been machined to within 0.002 inch. Metal plates, 0.062 inch thick were machined to the same nominal diameter, undertoleranced to 0.002 inch. The exact center is marked with a small conical blind hole so that a compass may be accurately located at center. These plates are checked to assure a close fit (by insertion in the counterbore), the loose ones discarded, and the remainder blued on the surface bearing the conical indentation.

The mask contour is then layed out on the blank, point by point, with a sharp scribe. These points are connected by a smooth curve, the actual mask outline. The computation of these points is based on equation (20), utilizing the photographic characteristics recorded in Figures 10 and 11. A summary of a typical set of these computations is shown in Table 1 which gives filter size and photographic data. This Table also summarizes the necessary formulas. It should be noted that

the choice of 270° for the maximum aperture angular opening is purely arbitrary; any other angle less than 360° would have sufficed. The choice of r_{max} is fixed by the size of the filter adapter and its corresponding frequency cutoff value. For the adapters made to fit these filters to the Image Enhancement Viewer, the effective diameter is 2.625 inches, corresponding to 100 lines/mm in frequency space. The last two columns of the Table are the basic data for mask layout.

A brief description of the procedure used for the preparation of Table 1 will illustrate how the mask outline is determined and serve as an example of subsequent mask calculations. $T(\bar{r})$, for the normalized coordinate system, is first computed. This constitutes the required filter radial transmission cross-section. This column is then converted to optical density, $D(\bar{r})$, by the standard formula shown in the listing below the Table. Using the appropriate curve in Figure 11, the exposure which produces this required density is ascertained, and becomes $E(\bar{r})$, or in terms of equation (20a), $g'[D(\bar{r})]$. Upon assumption of a maximum aperture angle, the constant, C, of equation (19) is computed. This is used to convert the exposure values into angles, $\Theta(\bar{r})$. The outline of the exposure mask computed in Table 1 is shown in Figure 12, a plot of columns 1 and 5 of the Table. The area within the outline is to be removed. The layout of the mask on the metal blank requires only that column 1 be scaled to the desired size. This is accomplished by the formulas listed, and shown in the last column of the Table.

3.3.2 Cutting out the Mask

In practice, when the mask layout has been completed, an additional 0.125 inch is added to the outer aperture edge to insure proper illumination at the filter edge. The mask is cut out with standard machine tools, and a file is used for finishing the curved portions to the proper shape. Approximately 0.004 inch excess is left around the critical central region to allow centering and adjustment within the exposure jig.

3.3.3 Centering and Adjustment

Because of the high cost and special surface of the High Resolution plates, less expensive Kodak 33 plates were used for the centering tests. These plates require less exposure, and develop to their highest contrast in Kodak D-11, at 69°F for five minutes.

The filter exposure mask is placed in the jig; an exposure is made. After processing, the center of the "filter" is examined. If a "density hole" appears, the mask shadow has covered the center of turntable rotation and more metal must be removed from the mask. If a dark "density spot" appears, the mask has had too much removed and the center of turntable rotation lies outside the mask shadow. Should a dark spot, surrounded by a ligher "density halo" appear, an off-center condition is indicated with the center of rotation just outside the shadow and to one side. This is the most difficult condition to correct since the direction of displacement is rendered ambiguous by the rotation of the plate. By interpreting such centering information, and removing appropriate thicknesses of metal with a jeweller's file, the mask aperture is ultimately adjusted to the proper shape. A final test is then made using a High Resolution Plate.

Once a satisfactory plate has been obtained, insofar as the center alignment is concerned, a microdensitometer trace is made. This checks the shape and helps determine the proper exposure. Should the trace indicate a deviation from the design shape, the mask may be filed or filled appropriately. A typical trace, after several shape corrections, is shown in Figure 13. This is the cross-section of the filter of Table 1. The ordinates of the trace may be converted to density with the aid of Figure 14.

The spike in the center of the trace of Figure 13 represents a small spot in the center of the filter. This is indicative of the size of the uncertainty in aligning the mask, and constitutes the fundamental limitation of this method of mask and filter manufacture.

Photographs of two exposure masks and the filters they produced are shown in Figure 15. The trace in Figure 13 was made of the filter shown in Figure 15a, experimental plate No. 178.

3.3.4 Cutting out the Filter

While the filter is made on a 4 × 5 glass plate, the Image Enhancement Viewer accomodates only a circular format. The circular filter must then be cut out and placed in a suitable adapter.

The presence of an emulsion will complicate cutting the glass, since the stress lines will not relieve through such a tough film. Further, commercially available cutting fixtures do not cut precise circles even under extremely well-controlled circumstances. Additionally, a means for assuring that the photographic and physical centers coincide must be provided. This requires a device for accurately centering the rectangular glass plate by use of the photographic density variation it contains. There is no assurance that the plates are located exactly the same on the exposure jig, so that mechanical centering is useless.

3.3.5 Cutting Jig

A device to accomplish the precise cutting was designed and constructed. The cutter of this device is a diamond, and can be adjusted for at least 0.50 inch on either side of the required filter radius.

Running vertically through the center is a hollow shaft. This is positioned over a small hole in the bottom plate, upon which the glass rests. Beneath this hole is located a photocell* whose output can be observed with a microammeter. When a microscope illuminator is placed over the hollow shaft, light reaches the photocell through the small centering hole. The illuminator is positioned so that the reading is a maximum. When the filter is inserted in the beam, the meter reading drops, and will be a minimum (for high-pass filters) when the filter is exactly centered. The filter position is adjusted accordingly, the source removed, and the glass scribed with the diamond. Photographs of the cutting device are shown in Figures 16 and 17.

After scribing, the now circular filter is taken from the rectangular glass by standard glass-cutting techniques. Rough edges are removed with a file. Edge polishing is optional. In practice, the glass used for making the High Resolution Plates is slightly brittle and a cleanly cut edge is difficult to achieve, especially with the restraining emulsion. Breakage (usually exemplified by the glass cracking across the circular scribe marks) is generally high.

3.3.6 Mounting

The filters, after cutting to a circular shape, must be mounted in adapters which can be installed in the Image Enhancement Viewer. The filters are mounted in adapters with a 60 per cent Harleco Synthetic Resin Xylene solution which hardens by solvent release. A photograph of a typical set of filters made for the Image Enhancement Viewer is shown in Figure 18. These in turn are mounted on the aperture wheel of the Image Enhancement Viewer. This installation is shown in the photograph of Figure 19.

Since the focus of the instrument will change when glass is inserted in the optical path, the occluding filters presently installed cannot be used without modification. However, by providing a disc of High Resolution Plate from which the emulsion has been removed, the focus will remain reasonably fixed when it is used in conjunction with the occluding filters. The image will be degraded, however, by the poor optical quality of the glass, and proper focus cannot be guaranteed.

---

* International Rectifier-Self-Generating Photocell, Mounted Cell #DP-5.

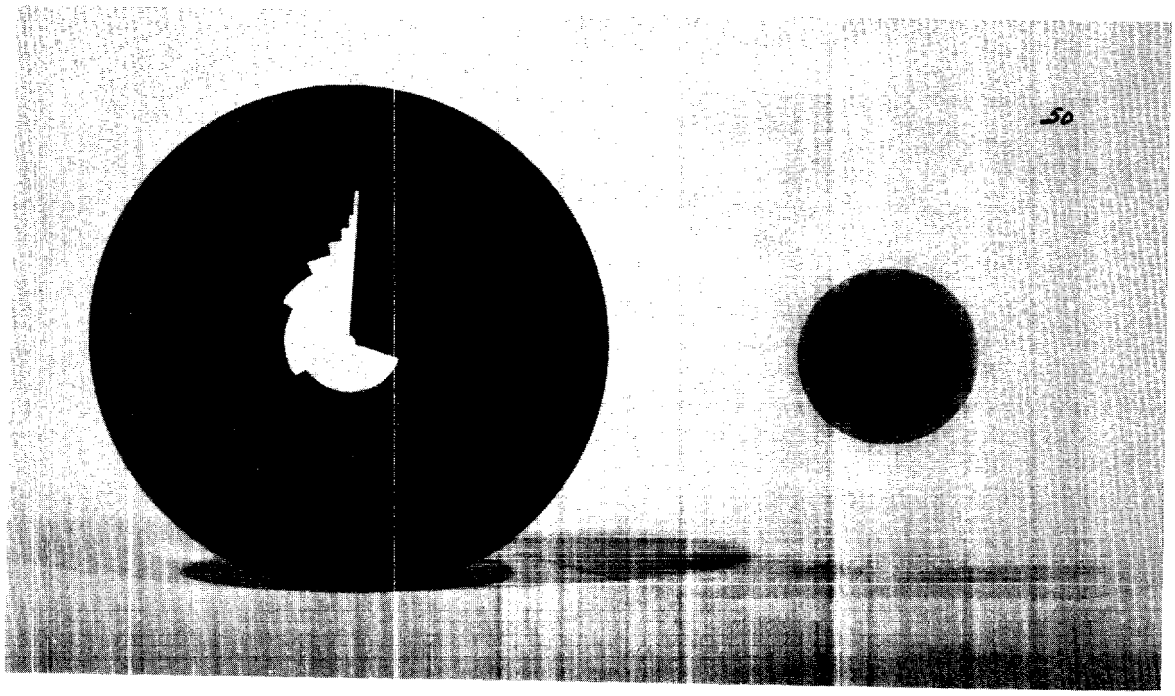

A. Geometric Mask; Plate developed in D-76, at 70°F, for 16 minutes 1787

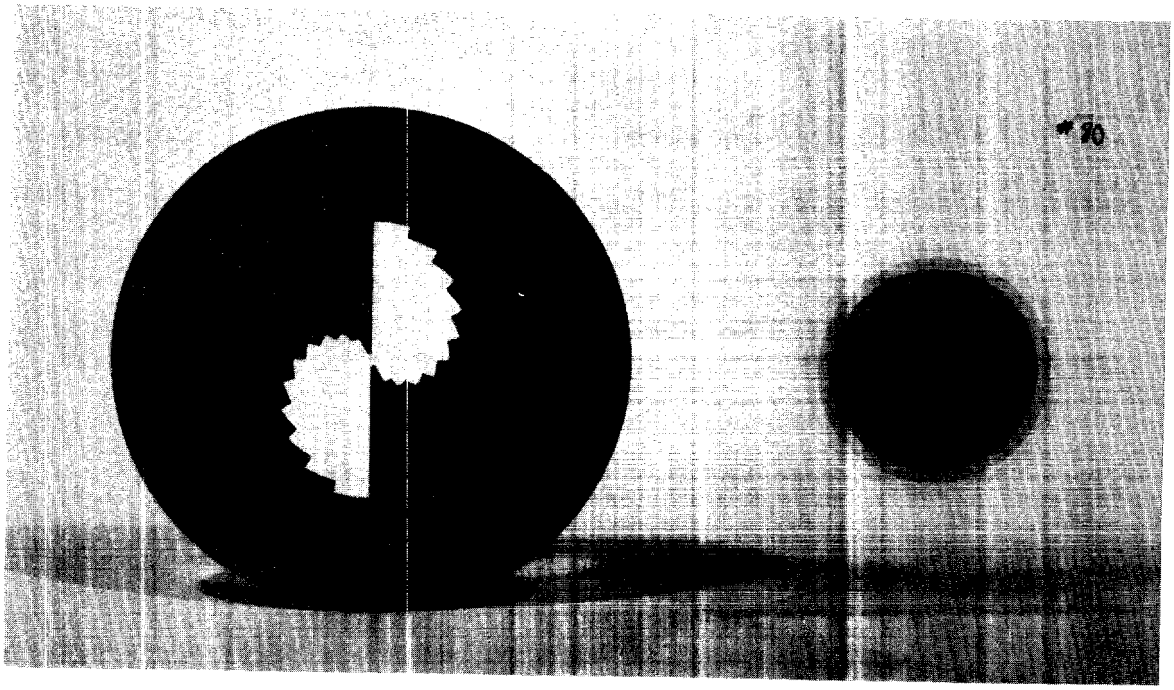

B. Arithmetic Mask; Plate developed in DK-60a, at 69°F, for 8 minutes 1787

Fig. 8 — Typical High Resolution Plate sensitometric test results with the masks through which they were exposed

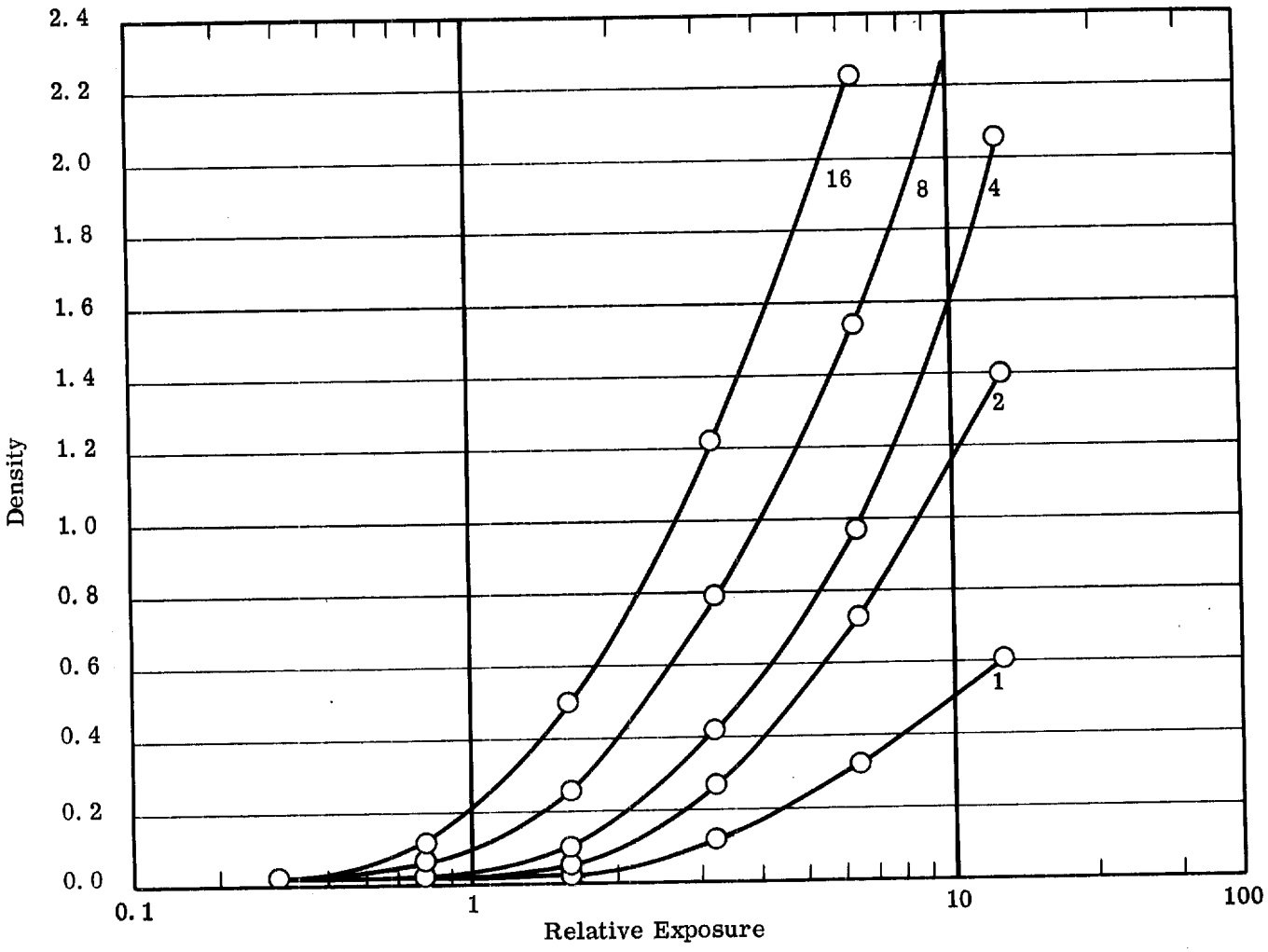

Fig. 9 — Sensitometric characteristics of Kodak High Resolution Plates developed in D-76 (2:1) under the specified exposure and processing conditions

Kodak High Resolution Plate

Development: D-76 (2:1), 70° continuous agitation, for times indicated (in minutes)

Exposed through Geometric Exposure Mask for 2 minutes at 15 volts, in Filter Exposure Jig.

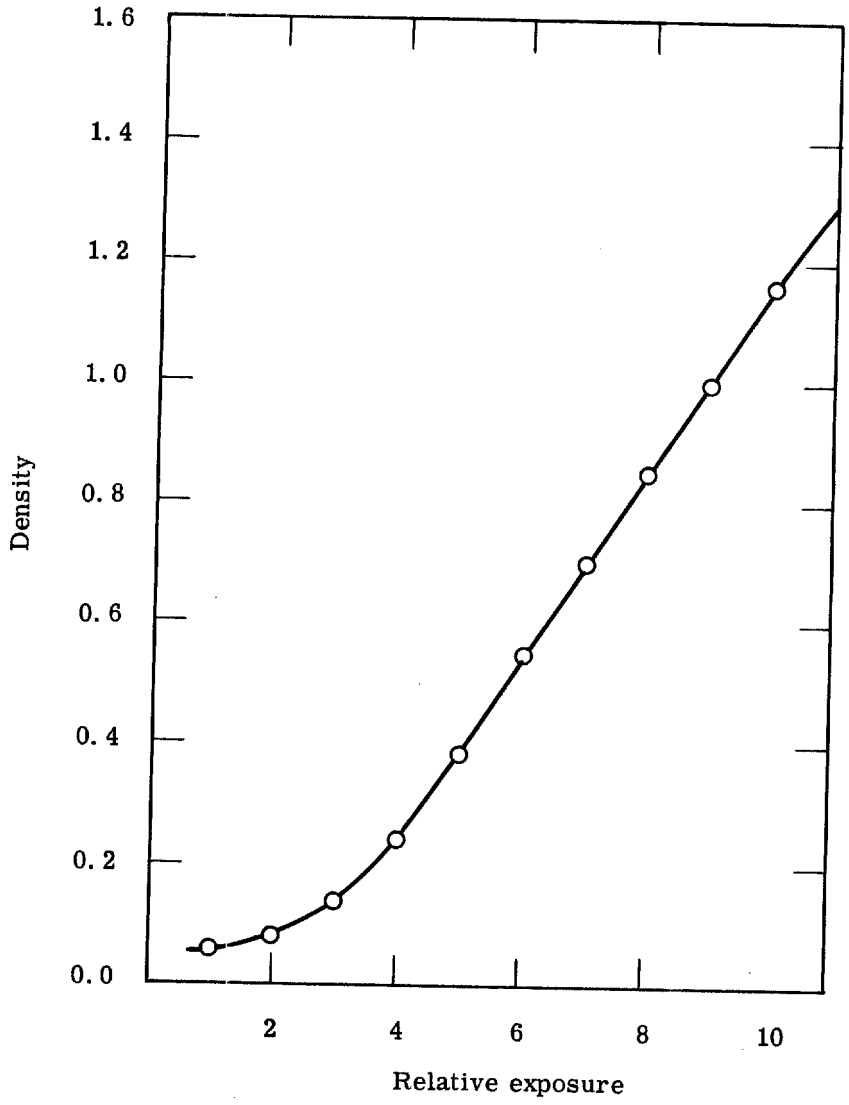

Fig. 10 — Linear sensitometric characteristics of Kodak High Resolution Plates developed in D-76 (2:1) for a specific exposure condition and one processing time

Kodak High Resolution Plates

Development: D-76 (2:1), 69°F continuous agitation, 16 minutes

Exposed through Arithmetic Exposure Mask for 4 minutes at 15 Volts, in Filter Exposure Jig.

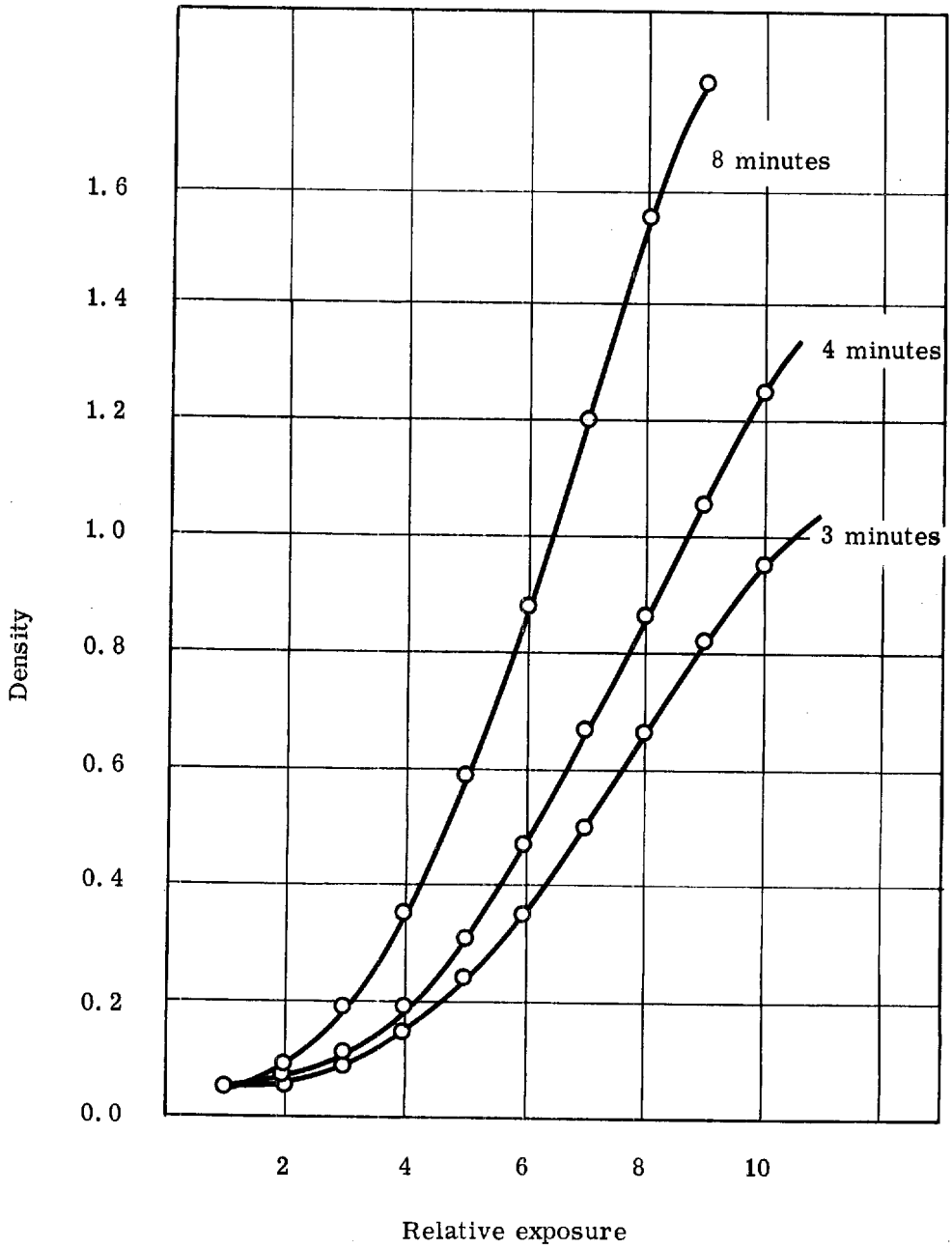

Fig. 11 — Linear sensitometric characteristics of Kodak High Resolution Plates developed in DK-60a under the specified exposure and processing conditions

Kodak High Resolution Plates

Development: DK-60a, at 69°F continuous agitation, for times indicated –

Exposed through Arithmetic Exposure Mask for 2 minutes at 17 Volts, in Filter Exposure Jig.

Table 1 — Computations for Gaussian Filter Mask No. 3

For: a = 8 $T_2 = 0.90$ $T_1 = 0.13$
DK-60a, 4 minutes, at 69°F (see Figure 11)

$\bar{r}$	$T(\bar{r})$	$D(\bar{r})$	$E(\bar{r})$	$\theta(\bar{r})$ (degrees)	r_m (inches)
0.0	.130	.886	8.15	270	0
.05	.145	.838	7.90	261.7	0.066
.10	.189	.723	7.35	243.5	0.131
.15	.257	.590	6.65	220.3	0.197
.20	.341	.467	6.00	198.8	0.262
.25	.433	.363	5.40	178.9	0.328
.30	.525	.279	4.85	160.7	0.394
.40	.686	.163	3.85	127.5	0.525
.50	.796	.099	2.80	92.8	0.656
.60	.857	.067	1.90	62.9	0.787
.70	.885	.053	1.30	43.1	0.919
.80	.896	.050	1.00	33.1	1.050
.90	.899	.050	1.00	33.1	1.181
1.00	.8999	.050	1.00	33.1	1.312

Summary of Formulas:

$$T(\bar{r}) = C_1 - C_2 e^{-a\bar{r}^2}$$

$$C_1 = \frac{T_2 - T_1 e^{-a}}{1 - e^{-a}} = 0.90026$$

$$C_2 = \frac{T_2 - T_1}{1 - e^{-a}} = 0.77026$$

$$\theta(r)_{max} = 270°$$

$$\theta(\bar{r}) = \frac{\theta(\bar{r})_{max}}{E(\bar{r})_{max}} E(\bar{r})$$

$$D(\bar{r}) = -\text{Log } T(\bar{r})$$

$$(\bar{r}) = r/r_{max}$$

$$r_{max} = 1.3125 \text{ inches}$$

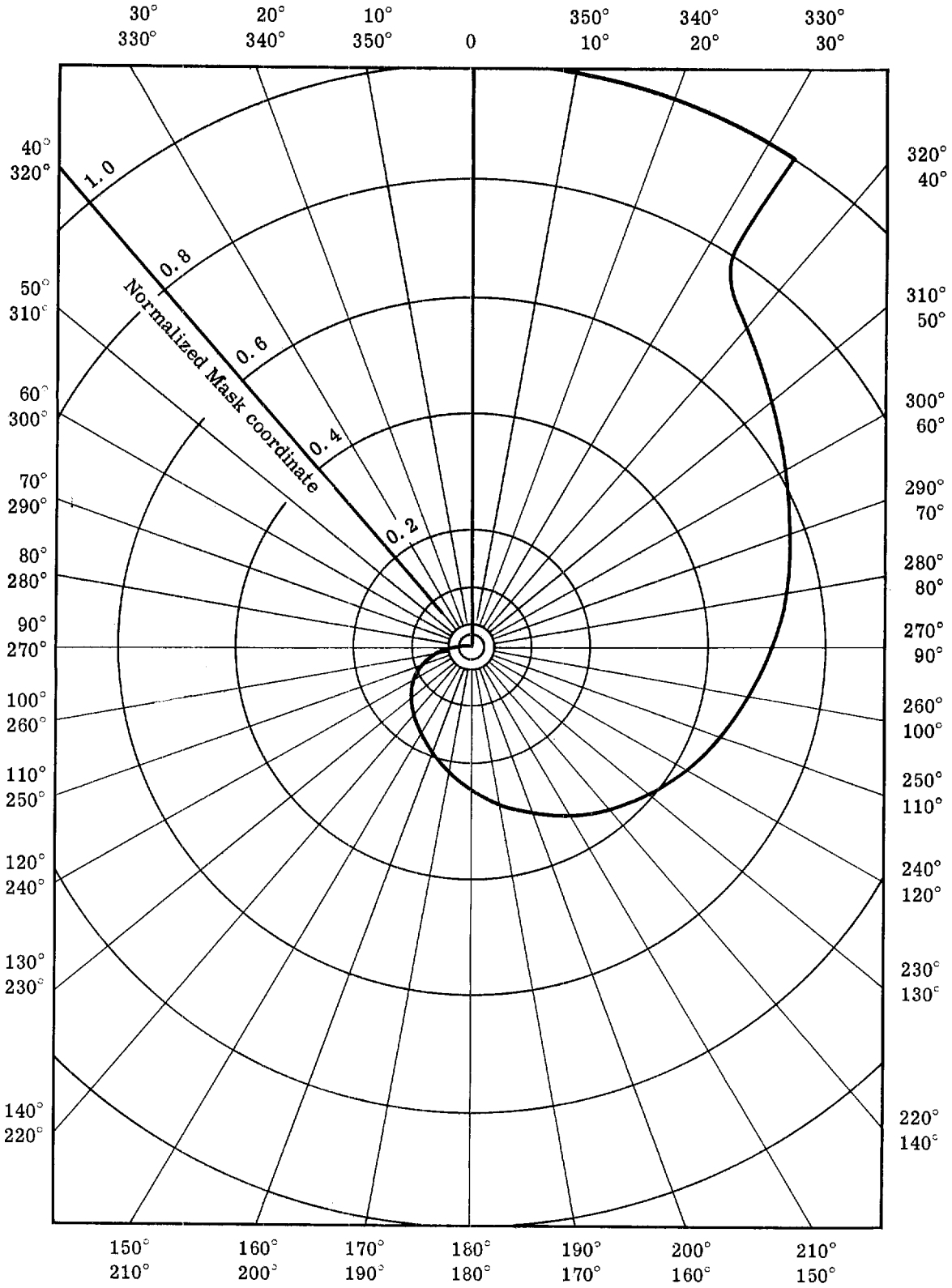

Fig. 12 — Outline of exposure mask aperture for producing Gaussian spatial filter No. 3, using normalized radius vector

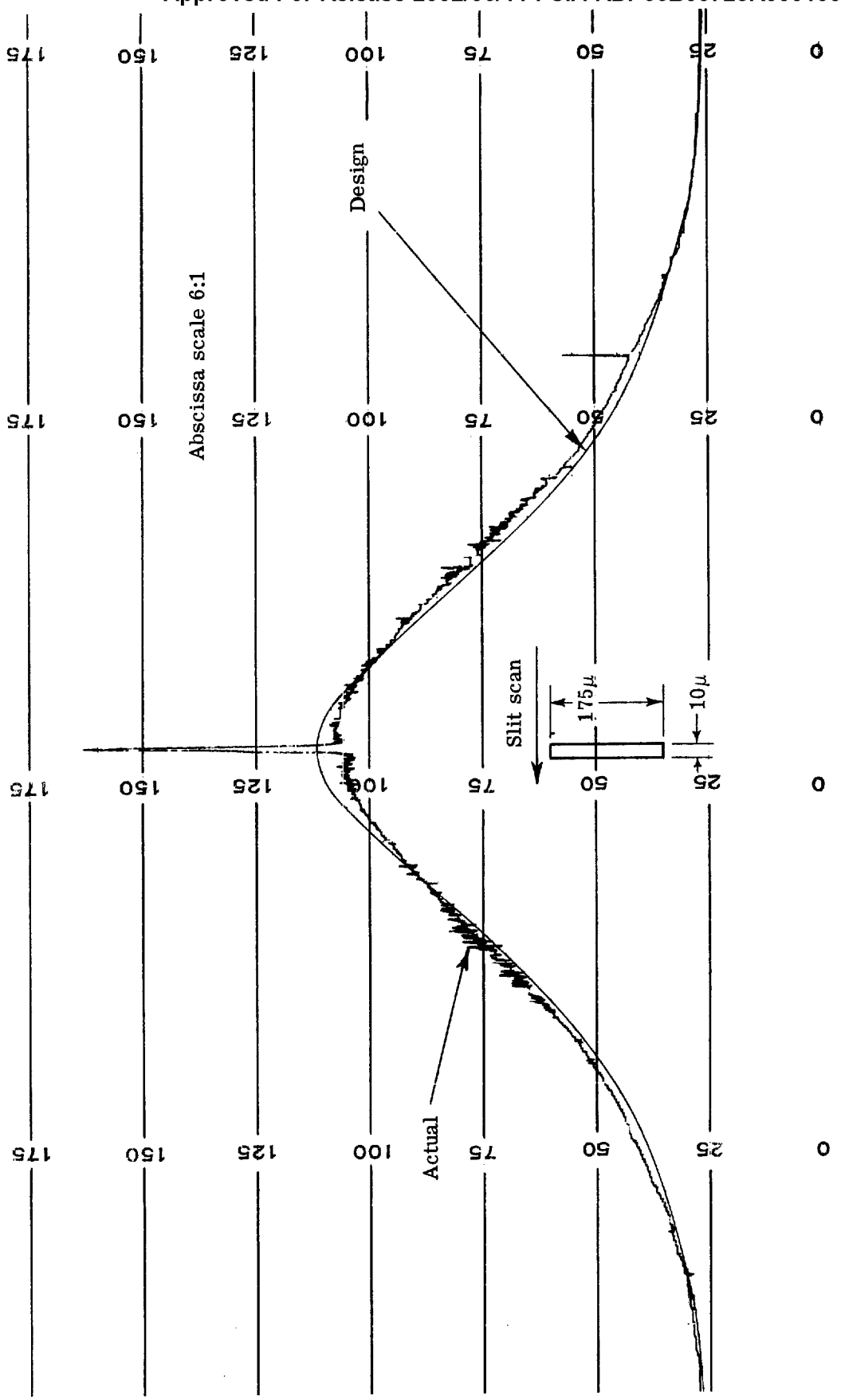

Fig. 13 — Comparison of design and actual Gaussian filter No. 3 cross sections

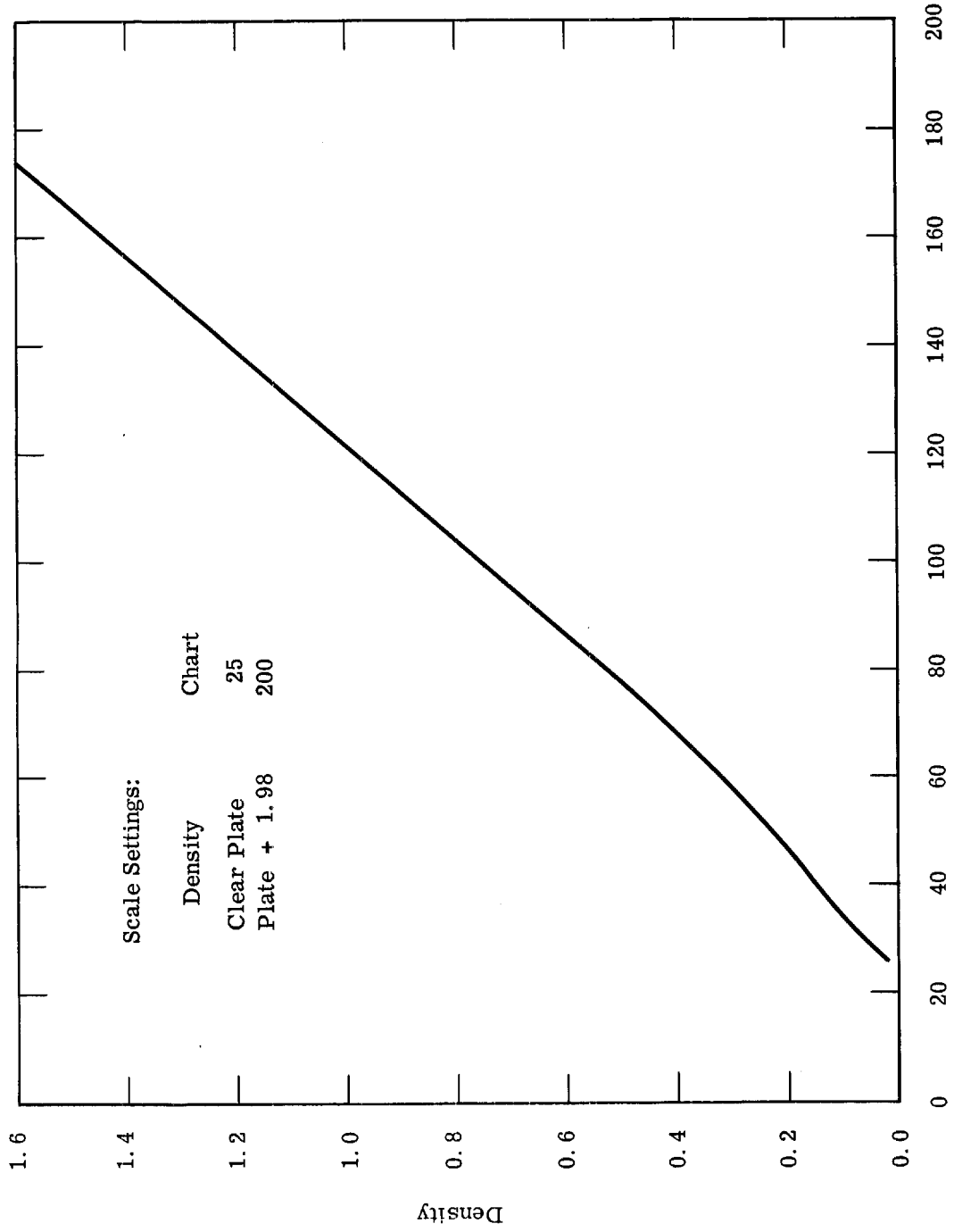

Fig. 14 — Calibration of microdensitometer and recording potentiometer, using cleared Kodak High Resolution Plate for the zero scale setting

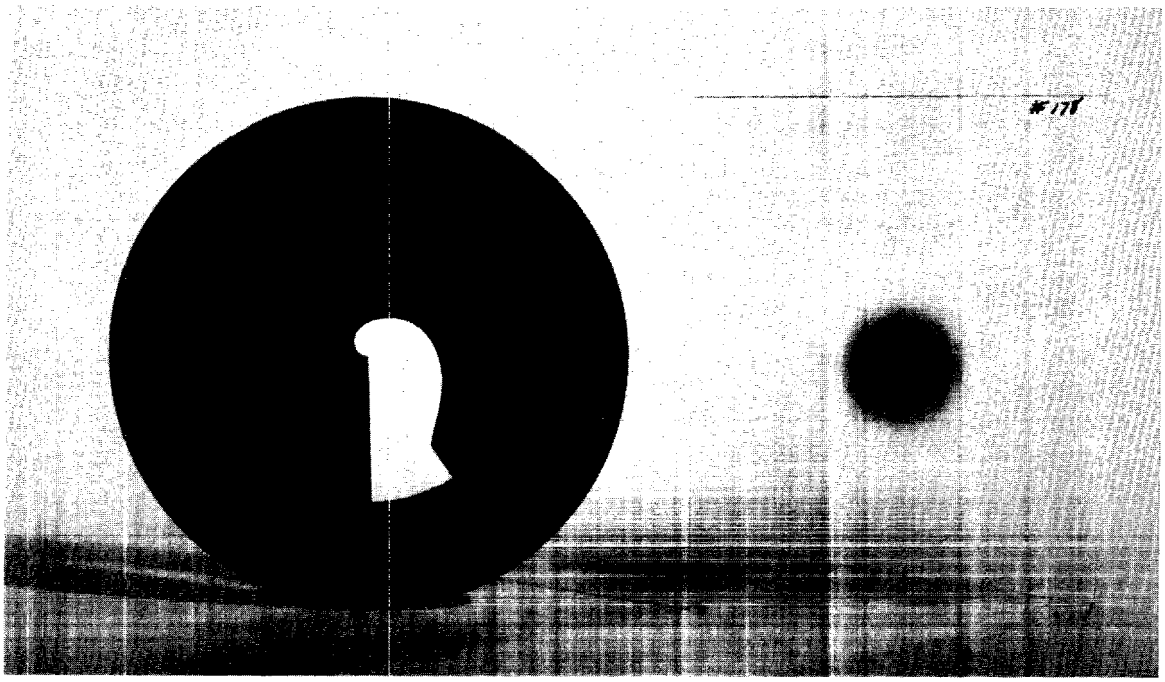

1832

A. Gaussian filter No. 3

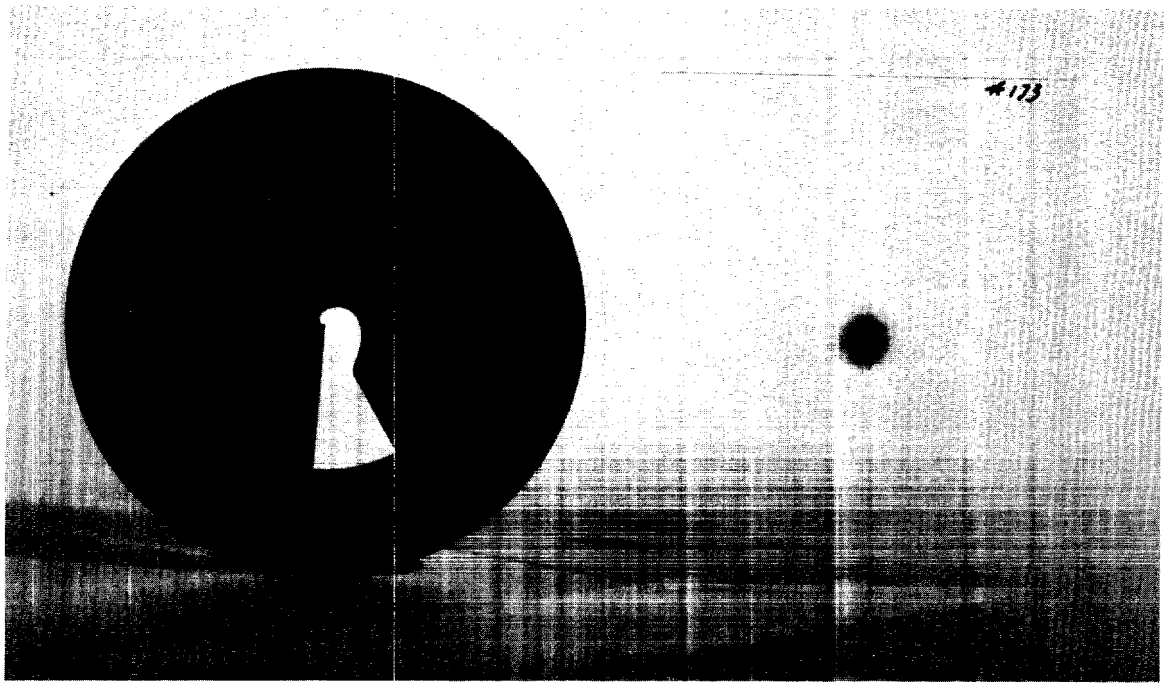

1831

B. Gaussian filter No. 4

Fig. 15 — Typical high-pass Gaussian spatial filters, with the exposure masks through which they were produced

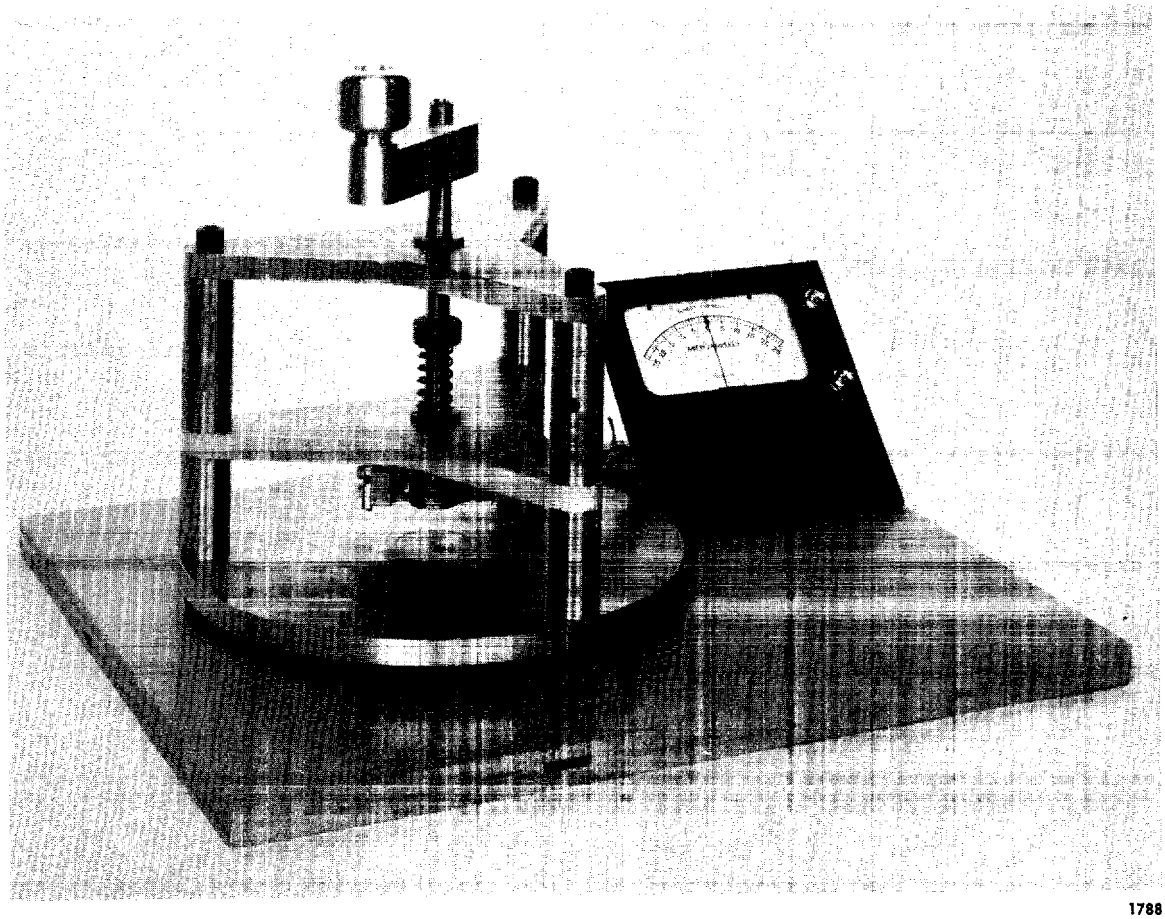

1788

Fig. 16 — Photograph of the Cutting Jig. The central shaft is hollow, and directly over the small hole in the lower plate. A microscope illuminator, set on the handle over the shaft, provides sufficient intensity to drive the meter needle off-scale

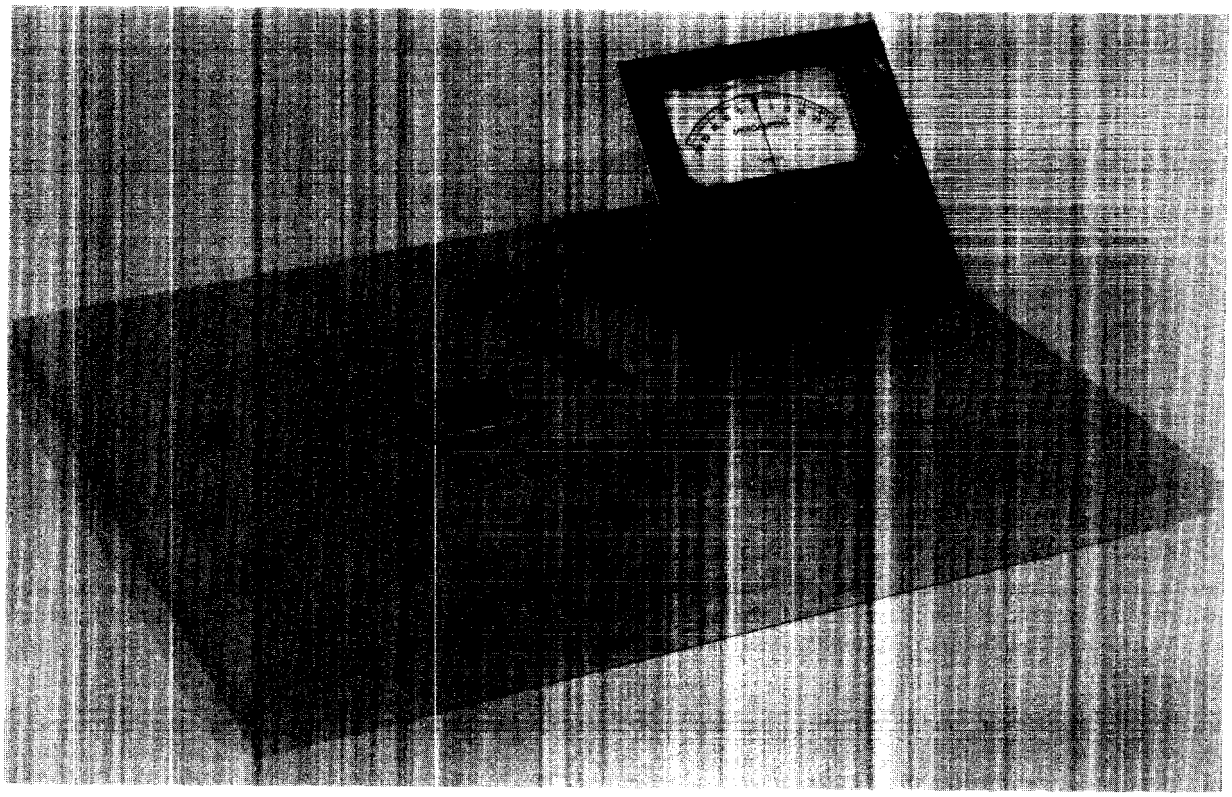

1790

Fig. 17 — Photograph of Cutting Jig base, showing the sensing device used for filter alignment prior to cutting. The bolt heads, spaced 120° apart, serve as locating studs to center Cutting Jig on base

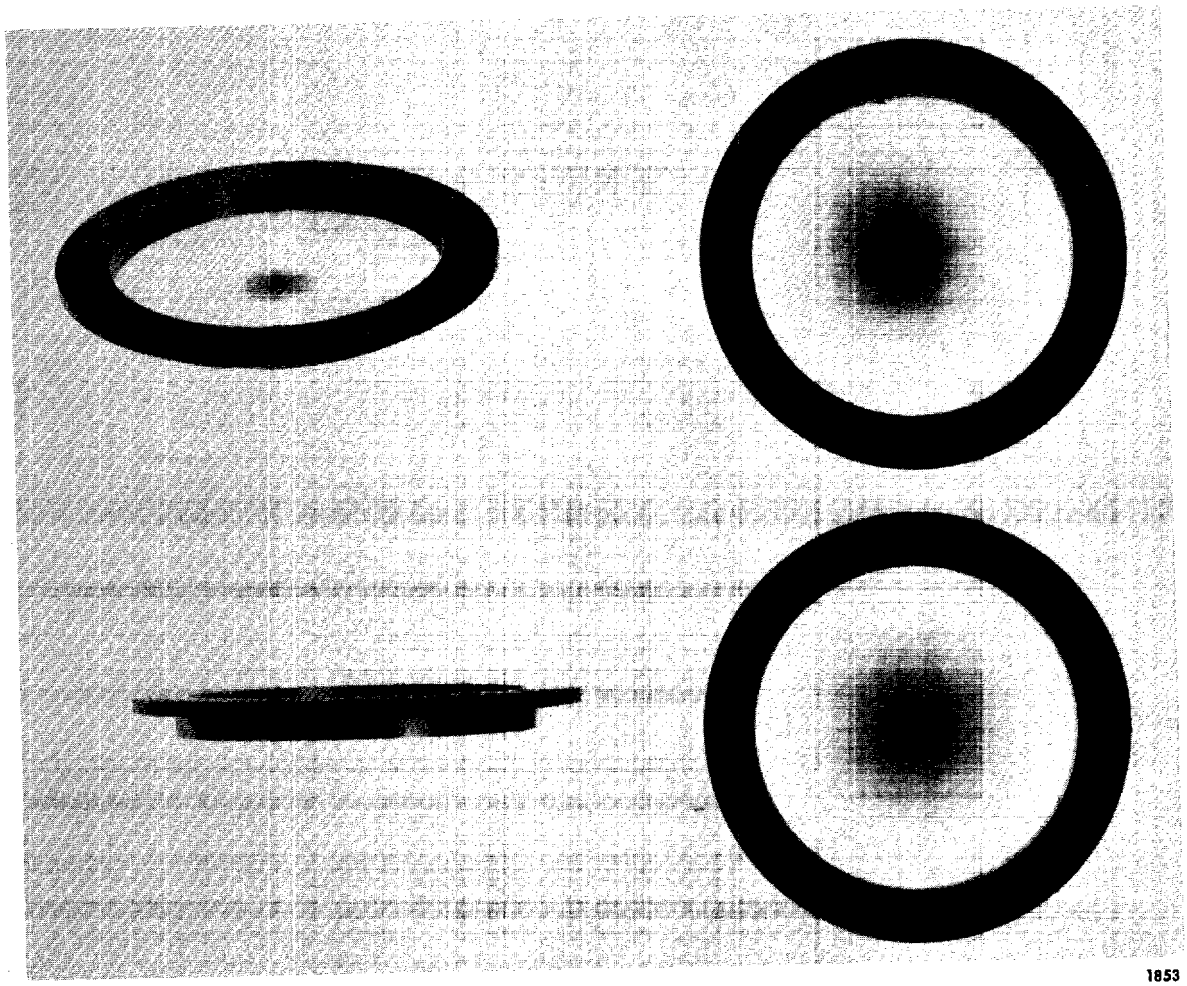

Fig. 18 — Gaussian spatial filters mounted in adapters for installation in the Image Enhancement Viewer. These are oriented to display the characteristics of the adapters

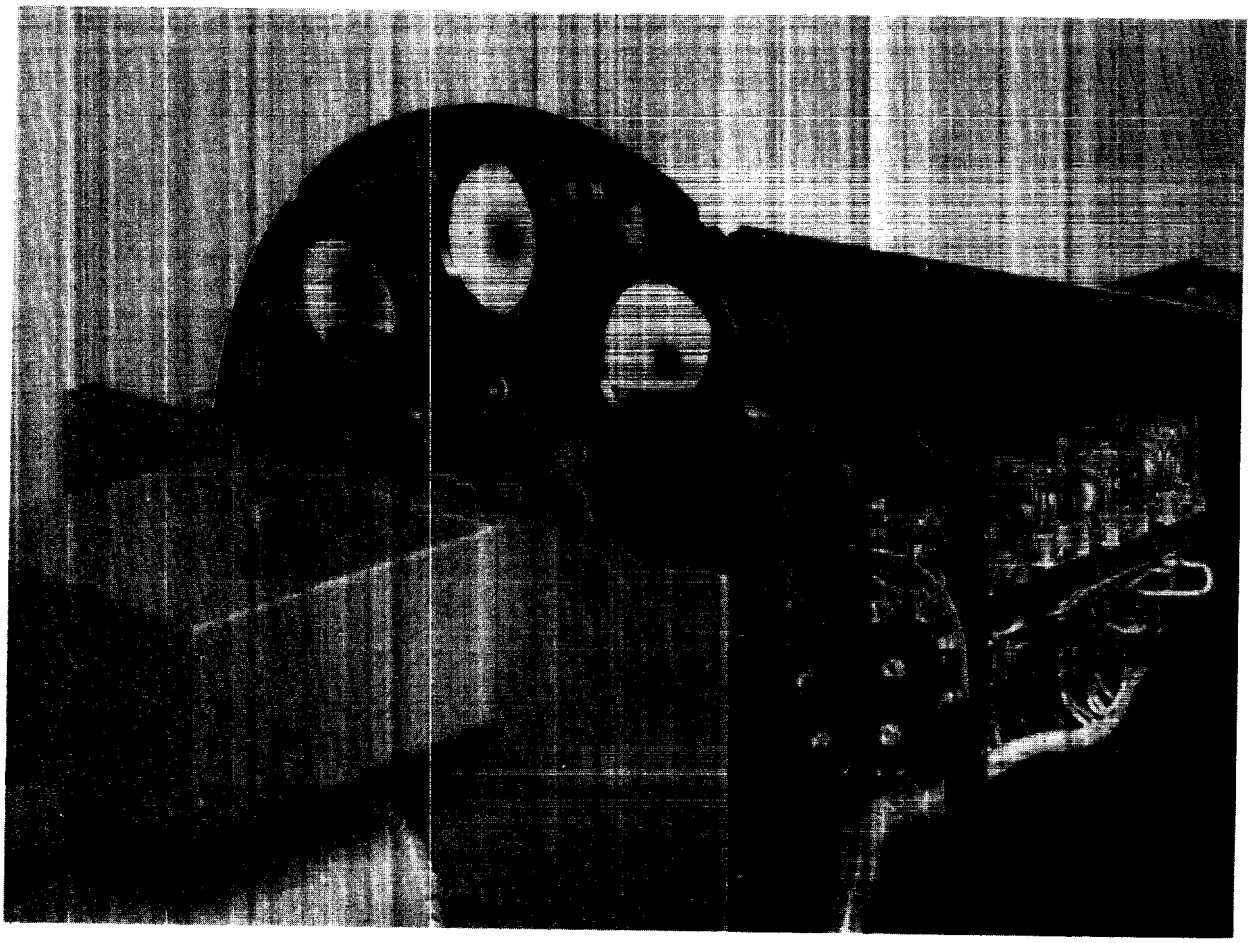

1852

Fig. 19 — Gaussian spatial filters installed on the Aperture wheel of the Image Enhancement Viewer. The wheel containing the occluding filters has been rotated out of normal alignment for this photograph, as evidenced by the displacement of the notches on the wheels.

3.4 PRACTICAL DESIGN OF GAUSSIAN FILTERS

3.4.1 Preliminary Considerations

The Gaussian spatial filter has been analytically described in equation (3). In a form suitably modified for analysis and subsequent computation, this equation is written

$$G(w) = \frac{T_2 - T_1 e^{-a}}{1 - e^{-a}} - \frac{(T_2 - T_1)\, e^{-a\bar{w}^2}}{1 - e^{-a}} \tag{21}$$

where

$$\begin{aligned} a &= \beta w_f^2 \\ \bar{w} &= \frac{w}{w_f} \end{aligned} \tag{22}$$

The relationship between $4\beta c$ and $(T_2 - T_1)$ has already been established in equation (11). The problem remains of associating the filter constants with pulse sizes to be encountered in typical aerial photographs so that a useful set of filters can be provided. The solution can be facilitated by knowledge of the proper values of the constant c, the pulse variance. [See equation (2)].

To obtain an approximate idea of the magnitude of c, consider the following. A set of square pulses (like the patters in a bar target) of periodicity k lines/mm has been degraded into a set of less sharply defined mounds of intensity (or density) of approximately Gaussian shape. Such a train and its resultant degradation is shown in Figure 20. Since the variance is a sufficient measure of non-sharp pulse width, the sharp and non-sharp pulse widths are related approximately by

$$\frac{1}{2k} \approx \sqrt{\frac{2}{c}}\ , \tag{23}$$

and

$$c \approx 8k^2. \tag{24}$$

Then, once the spatial frequency, k, is specified, it can be assigned a c which is, for all practical purposes, a reasonable measure of magnitude. Since the Image Enhancement Viewer has a practical frequency limit of 100 lines/mm due to the filter adapters, it will probably be of use to choose enhancement frequencies evenly spaced throughout the spectrum. Then a set of such frequencies which is by no means unalterable could be

$$k = 20,\ 40,\ 60,\ 80 \text{ (lines/mm)}. \tag{25}$$

Once the c's have been determined through equations (24) and (25), the a's may be calculated from (22), with the aid of

$$w_f = 2\pi k_f\ , \tag{26}$$

and

$$k_f = 100 \text{ lines/mm}. \tag{27}$$

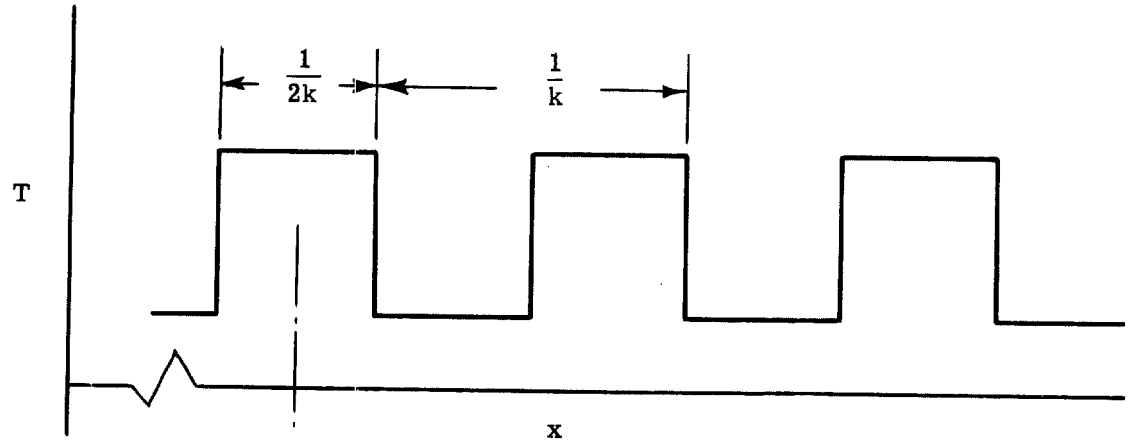

A. Spatial pulse train of periodicity k lines/mm.

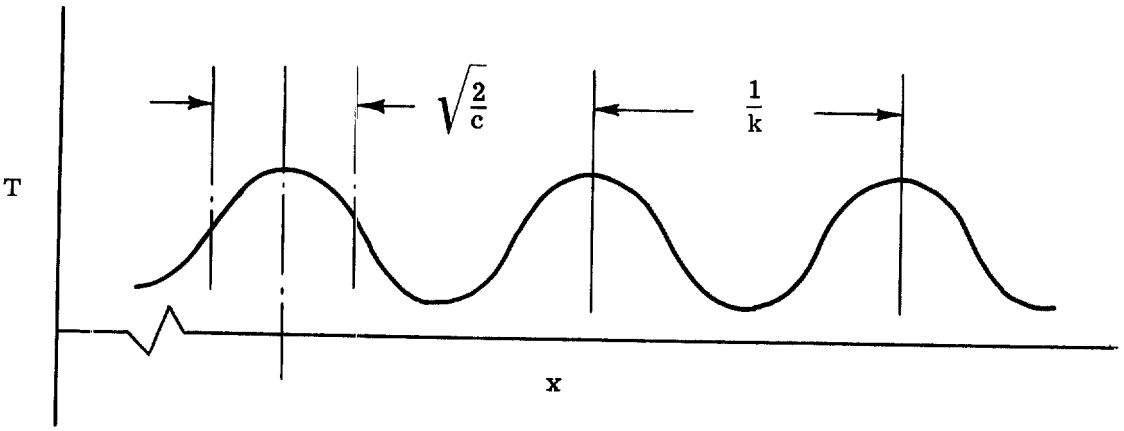

B. Degraded pulse train of periodicity k lines/mm, with pulse shapes approximately Gaussian in shape.

Fig. 20 — Assumed degradation of sharp spatial pulse train into train of approximately Gaussian shapes, with the parameters defined in terms of the periodicity

Following this, the transmission ratio, equation (11), must then be calculated for each $4\beta c$ product considered. Table 2 summarizes these computations for three values of $4\beta c$, utilizing the $\underline{k}$'s of equation (25).

3.4.2 Final Design Constants

Since the useful sensitometric limit on low density is 0.05 (see Figure 11), the quantity, T_2, is fixed for practical purposes at 0.90. For $4\beta c = \frac{1}{2}$, T_1 is then calculated to be 0.041, requiring an optical density of approximately 1.40. This lies outside the useful sensitometric range prepared for these investigations. This effectively eliminates the column of Table 2 which corresponds to $4\beta c = \frac{1}{2}$.

From the considerations associated with the development of the optimum constants, a pulse image which was narrower would be considered more suitable. Then computing the zero-abscissas for $4\beta c$ equal to unity and two, respectively, and comparing them, the zero for the former is smaller than that for the latter. This results in a higher peak value (and therefore a greater acutance, taking both considerations into account). This can be deduced from the behavior of the general curves of Figure 4. These results rule in favor of taking $4\beta c = 1$.

Filters having the characteristics shown in Table 3 have been chosen for fabrication, testing and evaluation in the Image Enhancement Viewer. They were based on the above considerations, but have had the values for $\underline{a}$ slightly changed from Table 2, to facilitate computation. The cross-sections of these filters are plotted in Figure 21, the abscissa referred to spatial frequency and scaled exactly for the Image Enhancement Viewer. These plots show the frequency attenuation which is to be applied in the plane of diffraction.

Table 2 — Summary of Preliminary Gaussian Filter Constant Computations on which Final Design Decisions Were Based

Enhancement Frequency, $\underline{k}$ (lines/mm)	$\underline{c}$ (mm^{-2}) $\times 10^{-4}$	a		
		$4\beta c = \frac{1}{2}$	$4\beta c = 1$	$4\beta c = 2$
20	.32	15.6	31.2	62.4
40	1.28	3.91	7.82	15.6
60	2.88	1.74	3.48	6.96
80	5.12	.98	1.95	3.90
$\left[\frac{T_1}{T_2}\right]_{opt.}$	—	0.046	0.142	0.363

Table 3 — Summary of Final Design Constants for Gaussian Spatial Filters

Filter No.	a	T_2	T_1
1	2.0	0.90	0.13
2	3.5	0.90	0.13
3	8.0	0.90	0.13
4	32.0	0.90	0.13

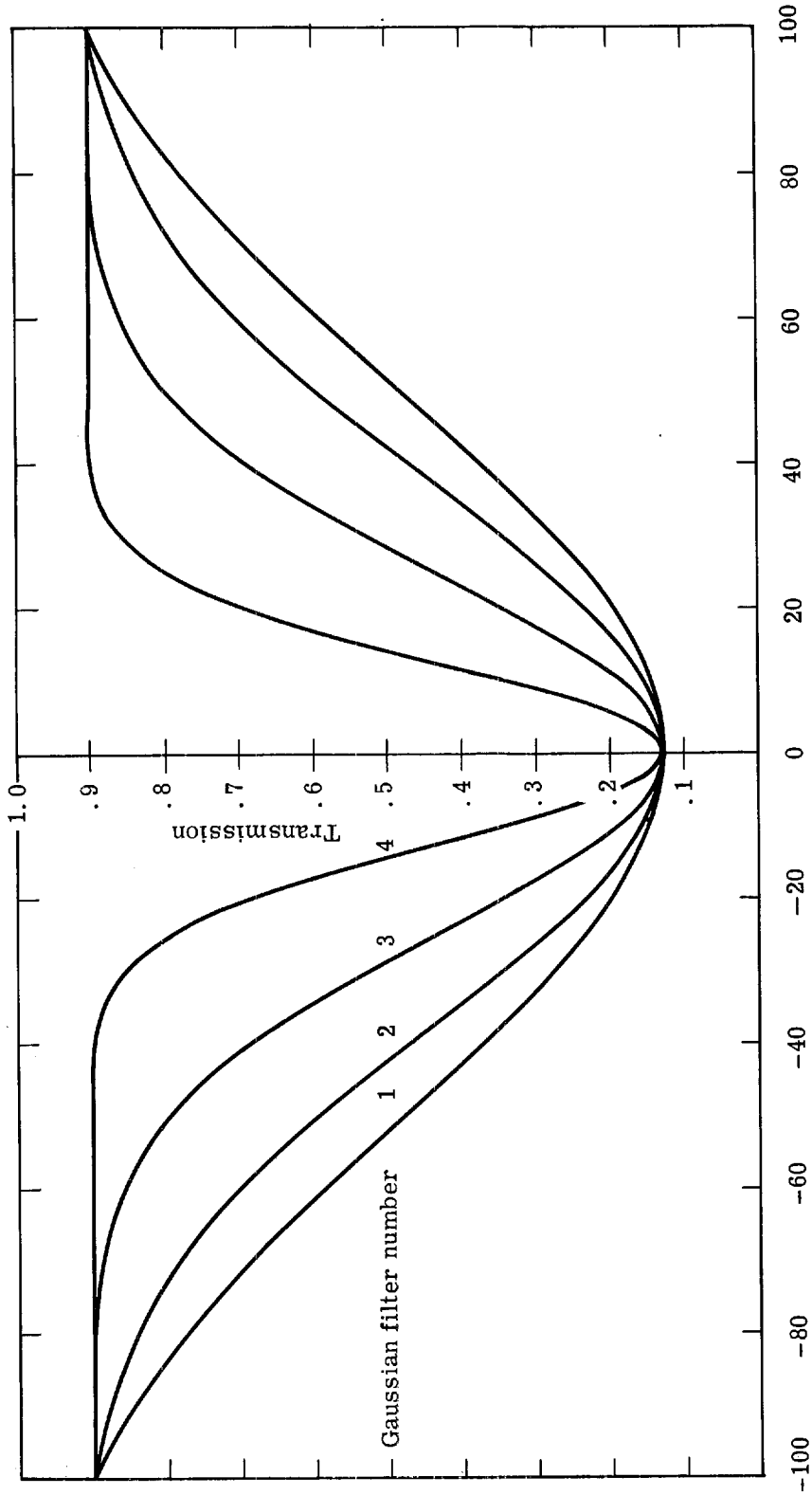

Fig. 21 — Design cross-sections of the fabricated Gaussian filters, showing the frequency attenuation produced in the optical system of the Image Enhancement Viewer

4. TESTING AND EVALUATION

4.1 PURPOSE

The tests and evaluation carried out for this research program served two purposes. Of primary concern, of course, was to achieve enhancement, or at least a demonstration of its feasibility. Of somewhat lesser importance was a quantitative evaluation of the glass used for the photographic plates, the effect on image quality of the glass bearing a photographic emulsion, and the resultant improvement (if any) obtained by laminating over the emulsion. It was known at the start that the glass would degrade image quality. Of paramount interest then, was the amount of degradation.

The tests reported here were carried out over the length of the entire program, and the results of each applied to subsequent stages of the research. For convenience, they have been combined and condensed in this single section. Additional testing was carried out during the course of the program. This considered problems of optical system vibration, attainment of best focus, temporary adaptation of the Image Enhancement Viewer to a 35mm format, and so forth. Since they have only a secondary bearing on the major concerns of the program, they will not be reported in detail.

4.2 PRELIMINARY MATERIALS EVALUATION

The purpose of these tests was to investigate image degradation due to the non-flatness of the glass used for the Kodak High Resolution Plates, and the non-uniformity of its photographic emulsion. The effect of lamination to improve these results was also to be considered.

4.3 TEST METHODS AND EQUIPMENT

These tests were carried out on the Spatial Filtering Test Bench, an optical bench developed at Itek, for precise, controlled experiments in a linear, coherent optical system. This bench contains an optical system identical to the Image Enhancement Viewer. Test results are directly applicable. The essential difference between the two is that the Test Bench operates with a 35mm format (using an Exakta VX body) and is vibration and shock isolated.

The test object was a reproduction of a USAF type, Buckbee-Meers sixth-root-of-two target, having a measured contrast of 13.7:1. This target, when examined in bluish light under a microscope, had a resolution limit of 204 lines/mm. The coherent optical system of the Image Enhancement Viewer, by virtue of its sharp cutoff at approximately 110 lines/mm, utilizes only part of the given target information. However, it does not attenuate frequencies below this cutoff limit. Therefore, use of this target permits testing and evaluation without the necessity of correcting results for systematic deficiencies. The object was immersed in a fluid gate to minimize coherence losses due to non-uniform flatness across the surface, and to hold it flat.

Best focus was obtained in the image (and focal) plane by using a 100× microscope. Each test was individually focused. The tests were made with the following placed in the diffraction plane, the ultimate location of the spatial filters:

1. Open aperture.
2. A clear High Resolution Plate, emulsion removed.*
3. Two emulsion-free High Resolution Plates laminated with Canada Balsam.
4. One unexposed High Resolution Plate, Cleared in Acid Fix.
5. An unexposed plate, cleared in Acid Fix, laminated to an emulsion-free plate with Canada Balsam.

Since the flatness of the plates, while staying within the Kodak specifications, varied from plate to plate, the test plates were chosen at random. Since this is the way the plates would be selected for filter fabrication, it was felt that choosing the "best" plates would not reflect the actual conditions fairly. Each test was made visually and the results recorded photographically for subsequent analysis. The film used for this record was Kodak High Contrast Copy, 35mm, processed in Kodak D-11 at 69°F for five minutes. Fixation was accomplished in Kodak Rapid Fix. Such a film type and processing would easily record as much detail as could be observed visually, provided the focus was correct.

4.4 RESULTS OF THE MATERIALS EVALUATION

Enlargements of the photographic records of the tests on the glass and emulsion are shown in Figures 22, 23, and 24. These figures are second-generation photographs of 15x enlargement, resulting in some loss in fine detail. Table 4 summarizes the photographic and visual resolution readings for these tests and should be examined in conjunction with the Figures.

The Table and Figures show that there is a definite degeneration of system response due not only to the glass but also to the presence of a non-uniform emulsion. The degradations of glass and glass with emulsion, while having approximately the same resolution limit, differ in their over-all quality.† The addition of an emulsion "smeared" the image considerably more, yet allowed spurious resolution to occur.

There was some optical power introduced by the glass as seen by the need to focus the horizontal and vertical lines separately to obtain the "best" focus, and evidenced by the resolution limits which differed according to orientation.

Examination of Figure 24 shows that the "ringing" is suggestive of a double image. This could have been introduced by a non-uniform phase shift due to the non-uniformity of the emulsion layer and/or the lack of parallelism of the two filter surfaces.

Laminating the plates, at least with Canada Balsam, does not contribute a significant enough over-all improvement to warrant further testing. A rather obvious improvement can be seen by comparing the bar corners in Figures 24a and 24b. The laminated plate shows much more sharply defined corners. The fundamental limitation of the lamination process is the glass quality, and since the flatness varies randomly, too wide a range of possible optical problems

---

*The emulsion was dissolved in an aequous solution of sodium hydroxide.

† This points up the difficulty of using resolving power, or resolution limit to specify image quality. Sine-wave response specification of such image degradation would serve a more useful purpose.

exists. It is entirely possible, for instance, to combine two pieces of glass whose flatness deviations coincide in such a manner as to introduce a large amount of optical power. While the effects of the emulsion have been definitely reduced, too many problems remain to consider lamination as a means for improving image quality with these plates.

4.5 EVALUATION OF THE GAUSSIAN FILTERS

Since the glass quality will degrade the aerial image, any quantitative evaluation of enhancement would be impossible. Quite obviously, the image passed through the clear aperture will be of better quality than that passed through the glass containing a filter. As a result, only qualitative studies were made.

The experiments were conducted on the Spatial Filtering Test Bench, which enabled use of the uncut filters (the filters still on the 4 × 5 glass plates). The test object consisted of a transparency made from an aerial photograph. The best image was obtained with the aid of a 50× microscope mounted on the rear of the camera and focused on the camera's focal plane.

Gaussian filters #3 and #4 were tested. In order to evaluate the resultant images, a photograph was taken through a cleared High Resolution Plate (emulsion removed) placed in the diffraction plane. As in previous tests, the image was refocused so that any change in glass or emulsion thickness would not affect the results. Kodak High Contrast Copy film was used and the processing carried out as in previous tests.

4.6 RESULTS OF THE FILTER EVALUATION TESTS

An enlargement (5×) of the photographic image obtained with the emulsion-free High Resolution Plate in the plane of diffraction is shown in Figure 25. Enlargements of the filtered images obtained with the Gaussian filters are shown in Figure 26.

Comparing Figures 25 and 26, there appears to be a definite enhancement of the fine detail. Note the details of the buildings along the main road; the shape of the buildings is sharply squared and the corners rendered more distinctly. Figure 27 contains microdensitometer traces of one of the buildings in this group, showing the relative contrast and sharpness improvement. These traces were made on the photographic images of the aerial photographs, enlargements of which are shown in Figures 25 and 26. *

The fine objects along the runway are vividly brought out, although not clearly enough to identify them without prior knowledge. It would appear that since the spread of the #3 Filter is larger than the spatial frequency content of the picture, the effect of enhancement is somewhat lessened. The degradation due to the presence of an emulsion and glass plate is clearly demonstrated, but does not hide the obvious improvement in acutance.

An enlargement of an image which has been passed through a sharp cutoff, occluding filter is shown in Figure 28. This affords a direct comparison of the two types of filtering, and

---

*The enhancement ideas developed in the theoreticial section considered aerial image intensity. It has been shown[1] that two carefully controlled photographic processes are required to render a photographic image linear with respect to aerial image intensity. Since the traces represent only one such process, direct linear assessment is impossible. However, since the ordinate scale is proportional to density, an approximation of image intensity can be achieved by inverting the trace and reading "intensity" for the ordinate.

permits a qualitative assessment of their relative effects. Each filter type has its particular usefulness, and concentrates its effects on different aspects of the image. Figure 28 exhibits the typical loss of image tone and shows the edge isolation characteristic of high-pass occluding filters. The Gaussian filtering of Figure 26 is much more subdued in its action on edges, but the complete tonal range has been preserved.

4.7 ADDITIONAL TESTING

During the course of the materials tests, it was discovered that the image plane of the Image Enhancement Viewer was undergoing vibration which blurred the horizontal groups of a bar target image at frequencies well below the system diffraction limit. In a successful effort to remove this undesireable image degredation, two steps were taken. First, the D. C. Power Supply* was removed from contact with the bench and a special table constructed for its support. Then, vibration damping pads † were inserted between the I-Beam and the wooden bipods, and between the bipods and the floor. These two steps removed the vibration effects, and it is recommended that the bench retain these modifications permanently.

An accurate measurement of the Image Enhancement Viewer optical system magnification was made. This was carried out by dimensional comparison of a test object with its photographic image on a precision Mann optical comparator. Within the tolerances with which a carefully handled photographic emulsion can maintain its dimensions, the system magnification is unity.

---

*This supply contains a cooling fan which is not vibration-isolated.

†" Vibra-Check", Lowell Industries, Inc., Boston 34, Mass.; supplied by the manufacturer, gratis.

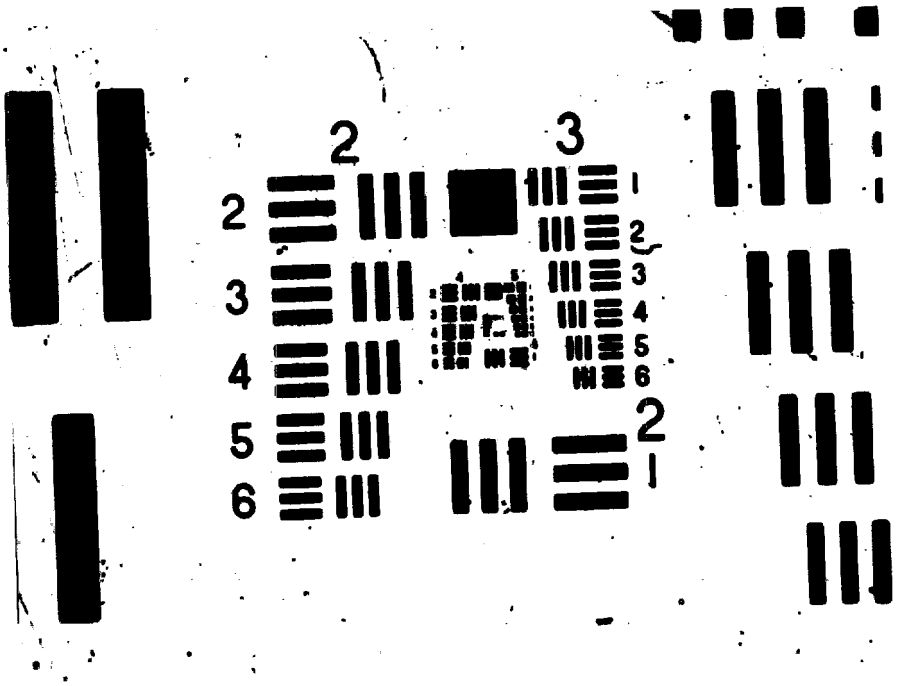

15×

Fig. 22 — Enlargement of the photographic image of a Buckbee Meers bar target observed on the Spatial Filtering Test Bench. It was imaged through the maximum system aperture, and the focus obtained with the aid of a 100× microscope. Scratches and other physical disfigurements are on the bar target object, and do not result from the imaging optics or subsequent photographic processes.

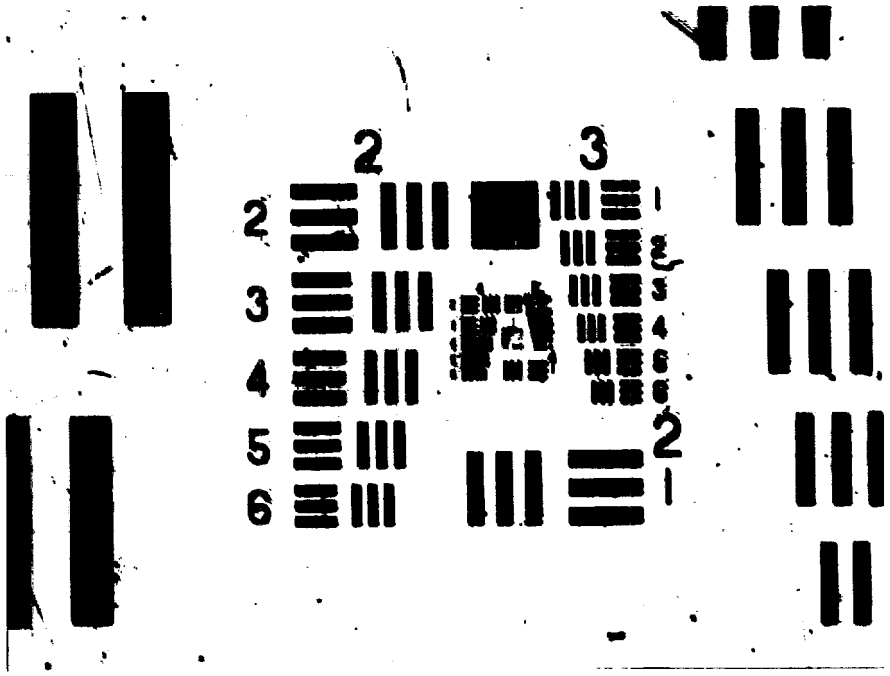

15×

A. One Kodak High Resolution Plate, emulsion removed, placed in the diffraction (filter) plane

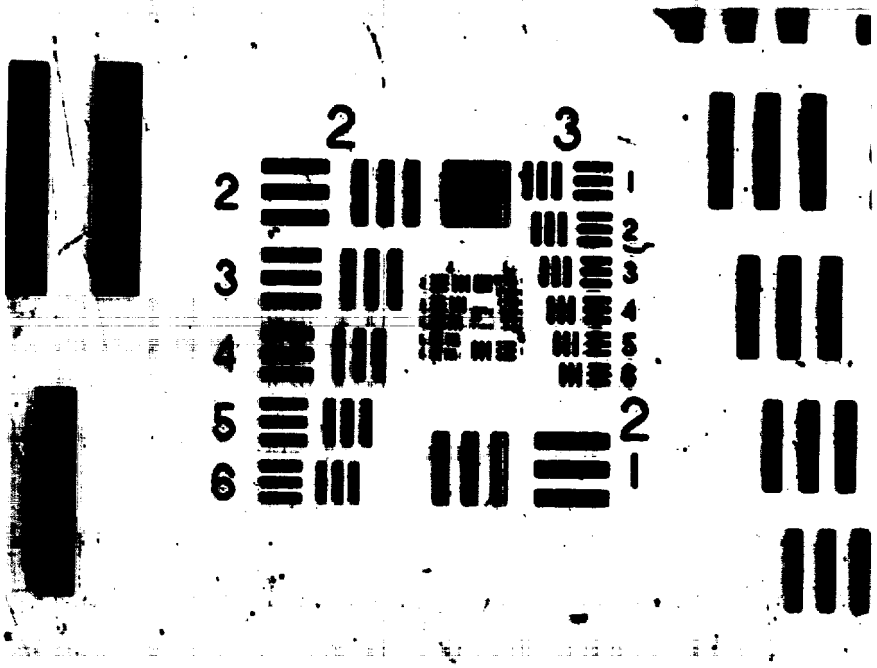

15×

B. Two laminated Kodak High Resolution Plates, emulsions removed, placed in the diffraction (filter) plane

Fig. 23 — Enlargement of the photographic image of a Buckbee Meers bar target observed on the Spatial Filtering Test Bench

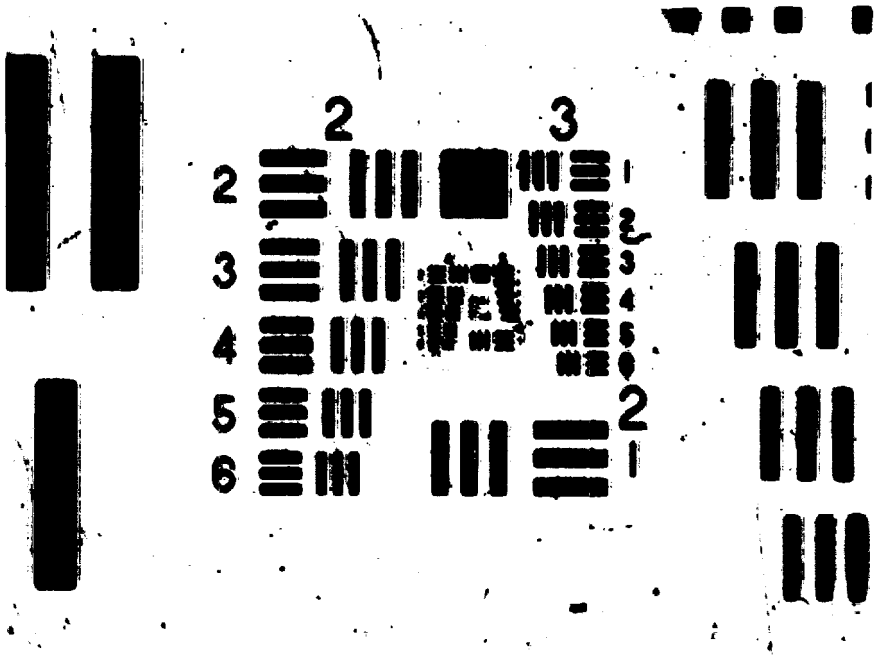

15×

A. One unexposed Kodak High Resolution Plate, cleared in Acid Fix, placed in the diffraction (filter) plane

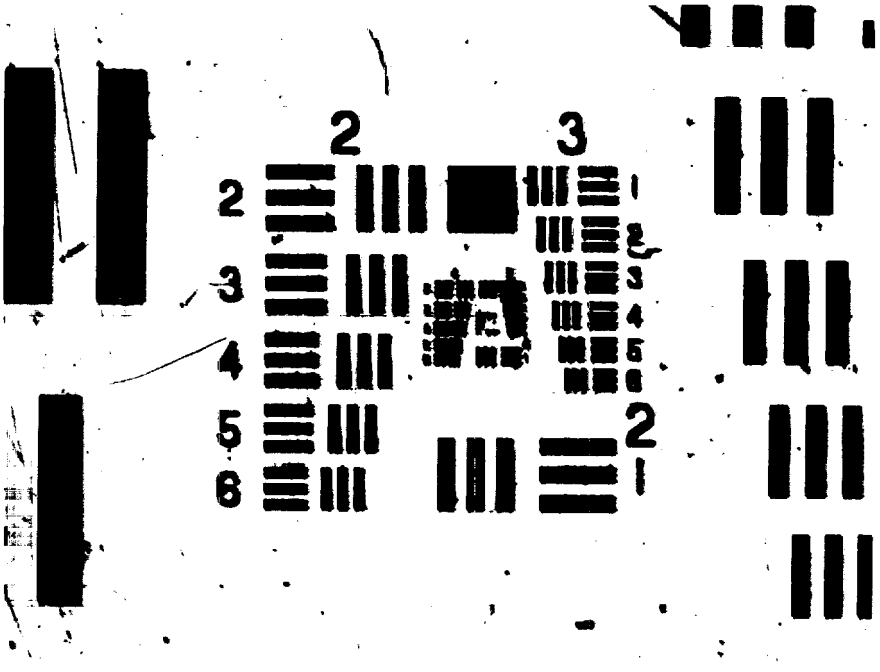

15×

B. One unexposed Kodak High Resolution Plate, cleared in acid fix, laminated to one High Resolution Plate with emulsion removed, placed in the diffraction (filter) plane

Fig. 24 — Enlargement of the photographic image of a Buckbee Meers bar target observed on the Spatial Filtering Test Bench

Table 4 — Materials Evaluation Data Summary

Figure No.	Condition at Diffraction Plane	Type of Test	Typical Resolution Reading* (lines/mm) in Coherent Illumination		Remarks
			Vertical	Horizontal	
21	Open Aperture	Visual	114	114	Reached maximum capability of system. There is a loss in resolution limit due to the photographic process and vibration. Image quality is excellent.
		Photographic	102	102	
22a	An emulsion-free High Resolution Plate	Visual	57	20.2	Visual test focused on vertical bars. Image quality greatly degraded; ringing along the bar edges observed. Quality varies with Plate orientation.
		Photographic	28.5	25.7	
22b	Two laminated High Resolution Plates (emulsions removed)	Visual	35.9	22.7	Ringing along the bar edges is amplified.
		Photographic	45.2	22.7	
23a	One unexposed High Resolution Plate, cleared in Acid Fix	Visual	40.3†		Over-all image quality greatly degraded. Response lowered.
		Photographic	45.2	35.9	
23b	One unexposed plate, cleared in Acid Fix, laminated to an emulsion-free plate	Visual	35.9†		Over-all image quality slightly improved over the unlaminated plate — see 23a.
		Photographic	32	35.9	

* Based on arbitrary position of plates in diffraction plane. Figures will vary from plate to plate, and for various orientations.
† Average reading of both horizontal and vertical bars, for several arbitrary orientations of plate.

Approved For Release 2002/06/11 : CIA-RDP66B00728R000100010021-5

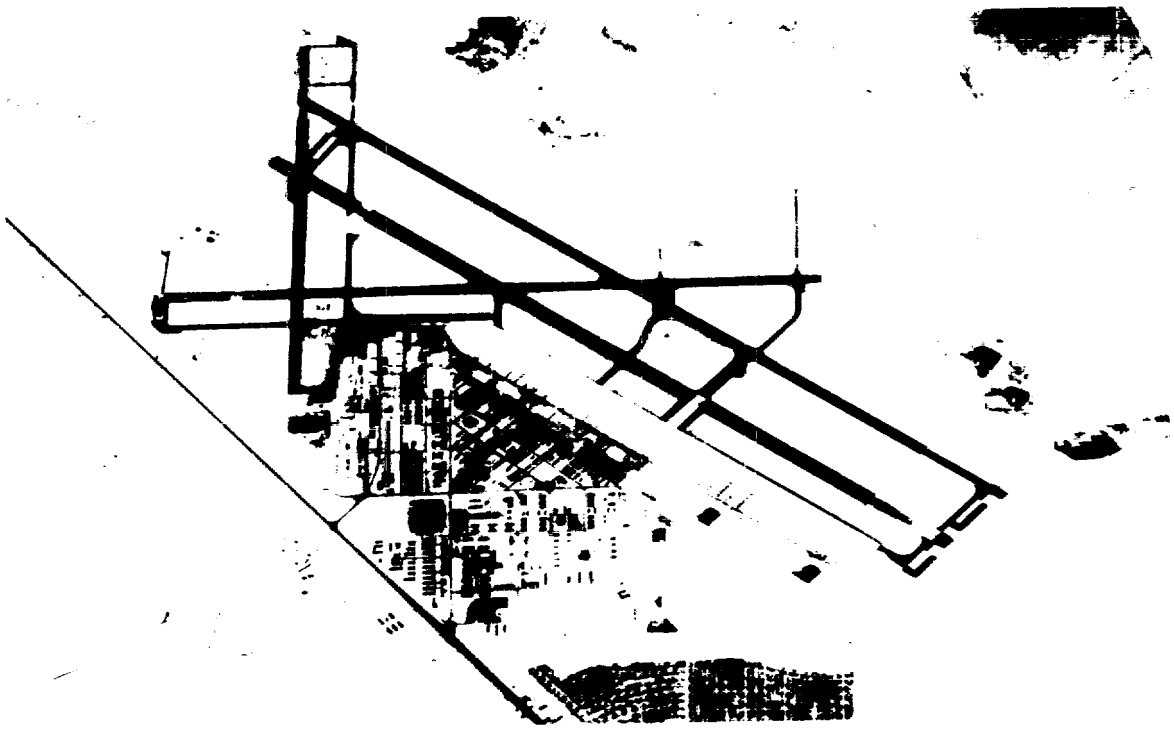

5×

Fig. 25 — Enlargement of an aerial photograph, the image of which was obtained on the Spatial Filtering Test Bench. One Kodak High Resolution Plate, emulsion removed, was placed in the diffraction (filter) plane to provide the basis for comparing this image with the photographs shown in Figure 26.

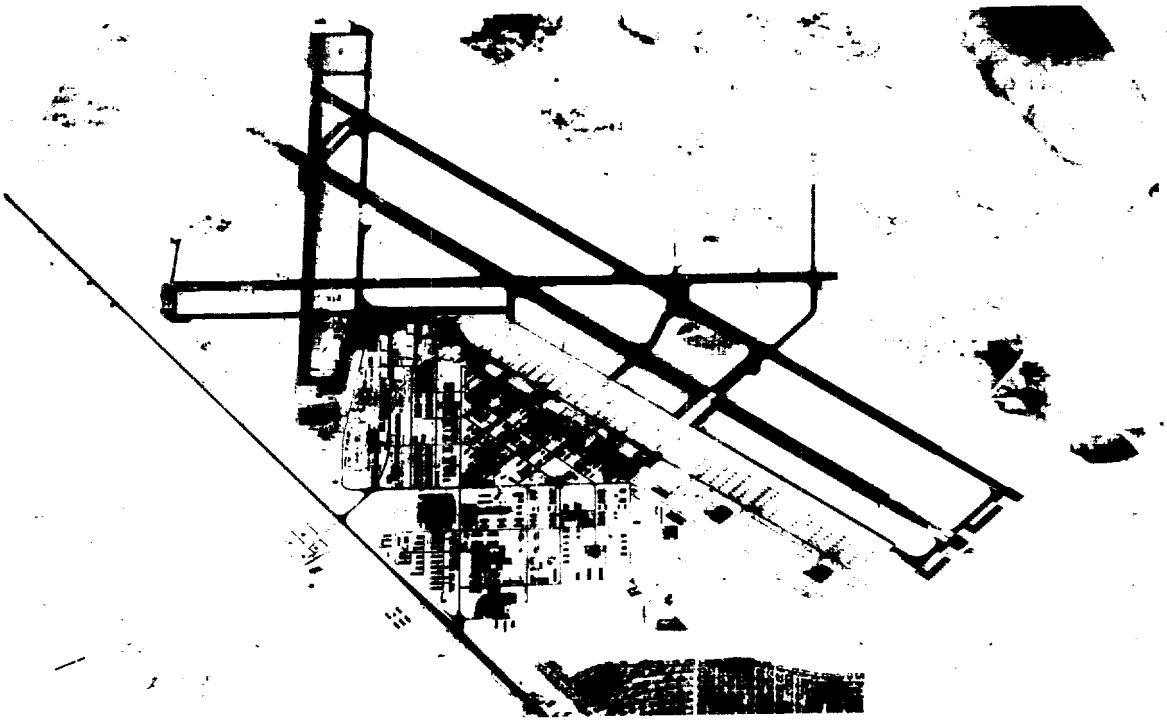

5×

A. Filtered with No. 3 Gaussian filter

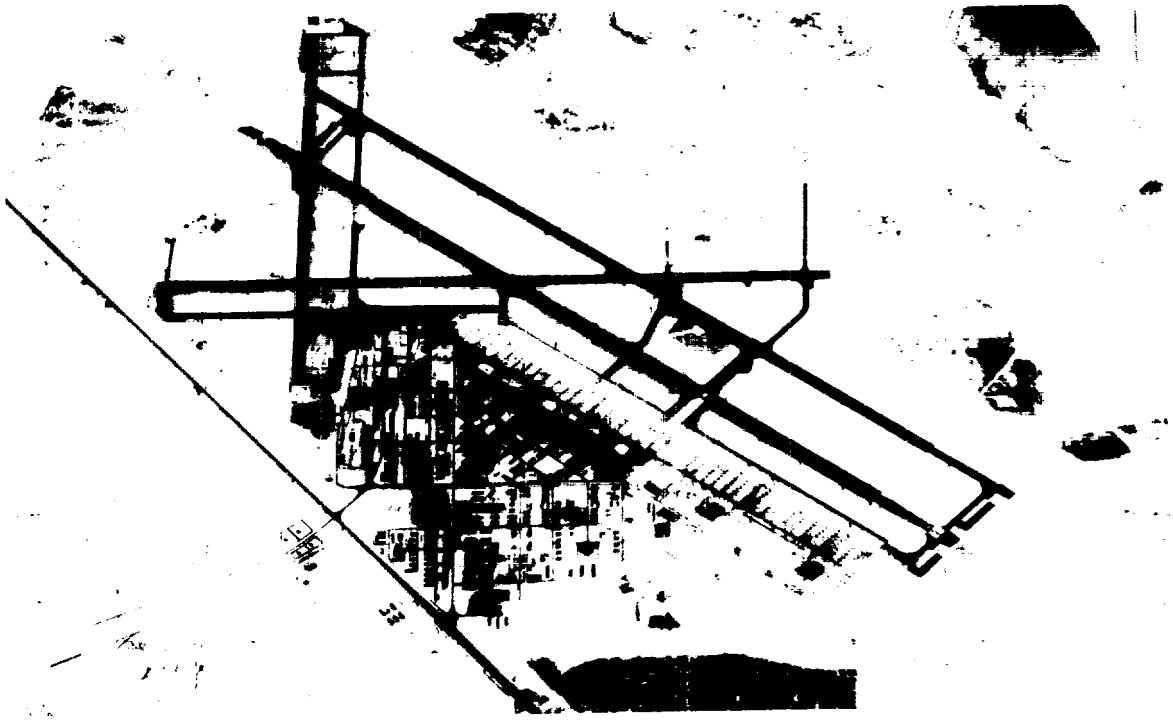

5×

B. Filtered with No. 4 Gaussian filter

Fig. 26 — Enlargement of an aerial photograph, the image of which was obtained on the Spatial Filtering Test Bench, for two specified Gaussian filters

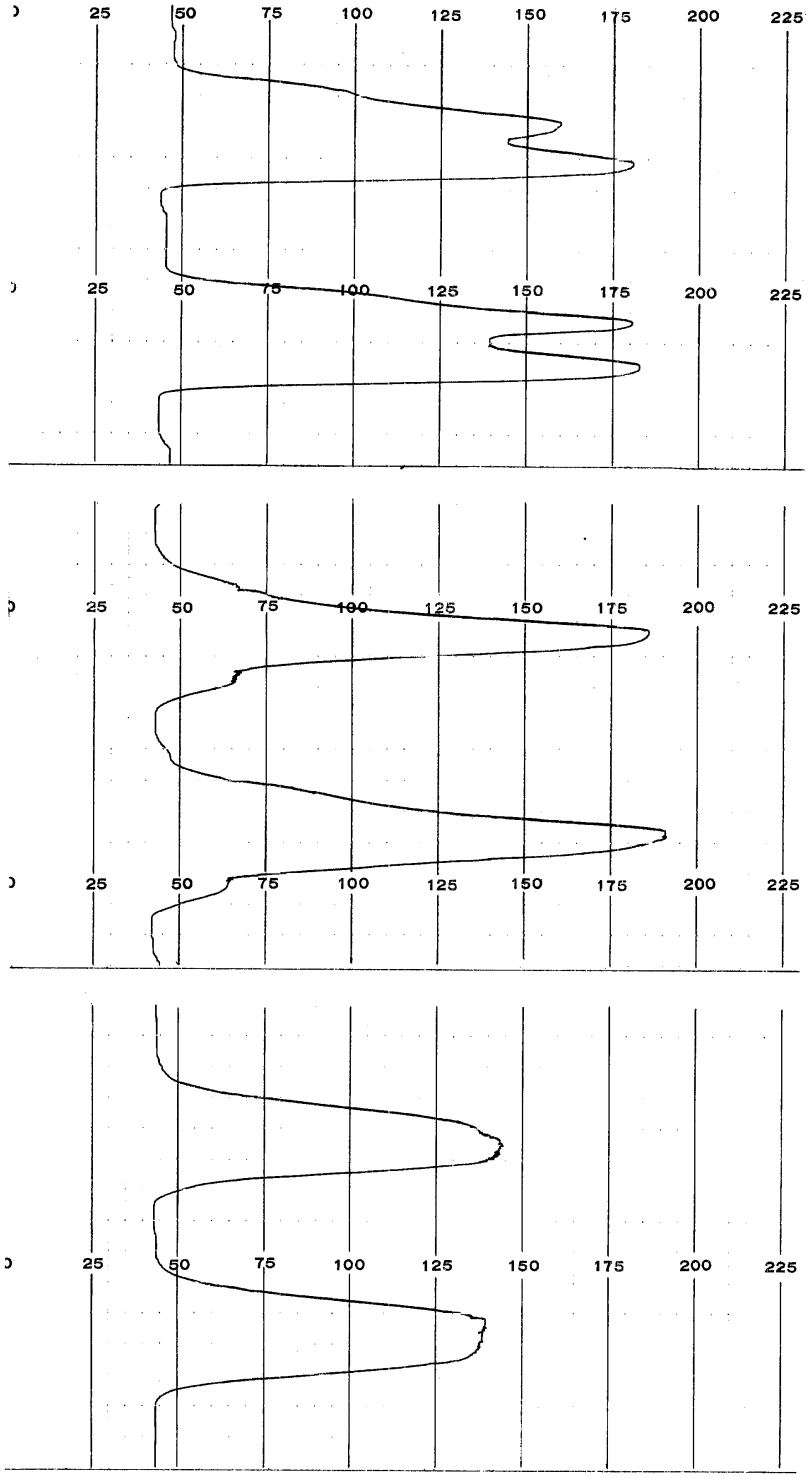

Fig. 27 — Microdensitometer traces of one of the buildings in the photographic images, the enlargements of which are shown in Figures 25 and 26. The inverted scale is an approximate measure of aerial image intensity, and the traces can be compared relatively

Abscissa scale: 1mm on image = 400mm on chart;
Slit width = 5 microns

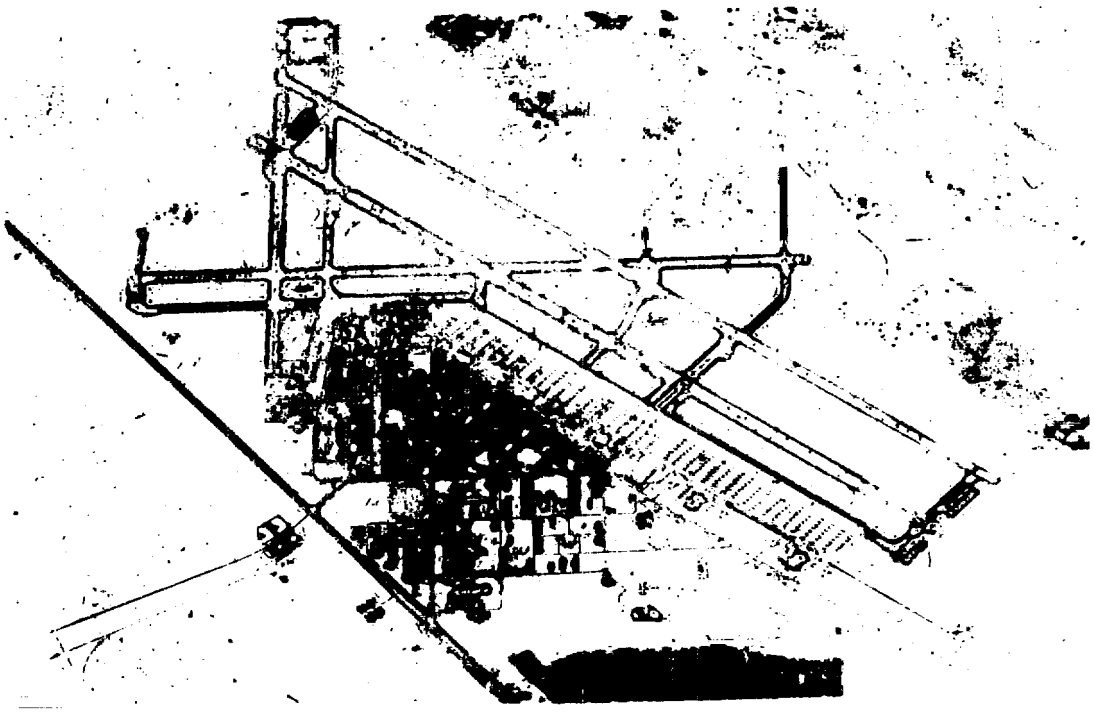

5×

Fig. 28 — Enlargement of the spatially filtered image of an aerial photograph obtained with the Image Enhancement Viewer. The image passed through a high-pass, sharp cut-off, occluding filter whose lower cutoff frequency was 3 lines/mm

5. DISCUSSION AND CONCLUSIONS

5.1 GAUSSIAN PULSE MODEL

The theoretical developments show that a Gaussian pulse model can be enhanced (its acutance improved) by use of a high-pass Gaussian spatial filter. Controlled experiments to verify these predictions were not carried out, primarily due to lack of properly prepared test objects. However, the aerial photographs of Figures 24 and 25 provide a qualitative verification. In the lower left-hand section of Figure 24, there appears a small road which leaves the large main road at right angles. The small width of this road and the indistinctness of the edges provide a close approximation to the Gaussian pulse. Figure 29 shows three microdensitometer traces of the photographic image transparencies of approximately the same part of this road. The first of these has not been filtered, and its cross-section looks quite like the nonsharp pulse of the theoretical studies. The second and third traces were obtained from the images which had been passed through the Gaussian filters #3 and #4, respectively. Comparison of these "pulses" shows an increase in contrast in a manner predicted by the plots of Figure 4, although the center trace appears to be from a section of the road not quite the same as the other two.

While this is hardly conclusive proof, it does indicate that the nonsharp pulse model has a reasonable verisimilitude, and warrants further experimental study. Such a model can serve a useful purpose in that spatial filter types may be tested "against" it, through equation (8), and enhancement ascertained analytically.

5.2 ENHANCEMENT WITH GAUSSIAN FILTERS

The photographs of Figures 24 and 25 indicate the degree of enhancement which can be expected with the Gaussian spatial filters. The effects are very subtle, unlike the dramatic changes effected by the sharp cutoff, occluding filters. The desired image tone has been preserved as expected, and the regions of fine detail (edges, building shapes, etc.) have all been raised in contrast and sharpened. Within the obvious restrictions of the degradations caused by the glass plates, frequency attenuating filters have definitely proved capable of enhancement.

5.3 FILTER MANUFACTURE

The method of filter manufacture appears practicable, within the limitations of the inherent reproducibility tolerances of the photographic process. The average number of plates rejected for each one accepted was 15. Rejections resulted from improper exposure (usually due to lamp brightness fluctuations caused by local power drains), pinholes and other emulsion imperfections, and minute misalignments of the exposure mask. Because of the required tolerances on the mask blank, identical replacement of the exposure mask was impossible. This caused

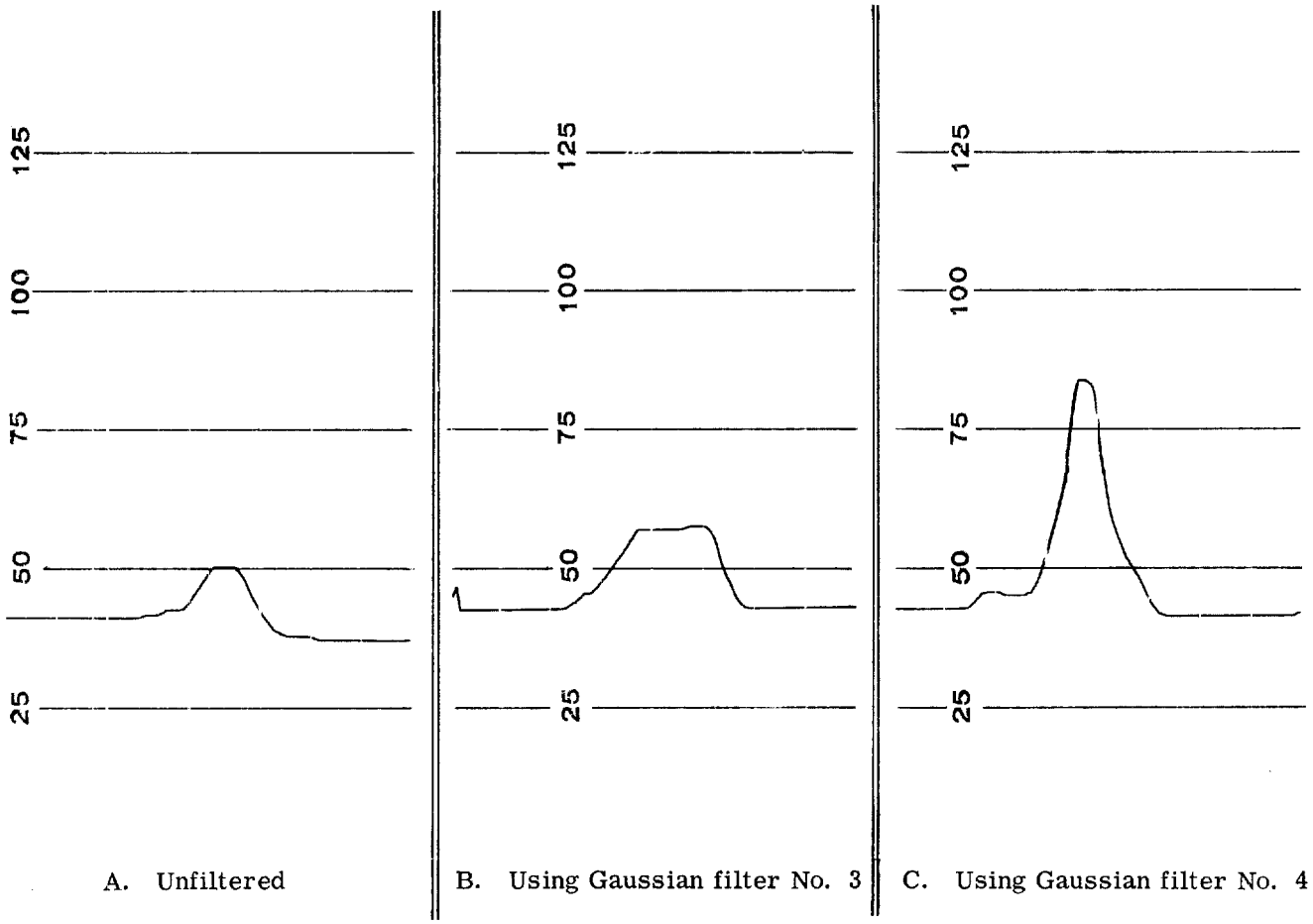

Fig. 29 — Microdensitometer traces of one of the roads in the photographic images of the aerial photographs, the enlargements of which are shown in Figures 25 and 26. The ordinate is an approximate measure of aerial image intensity; the traces can be compared relatively

Abscissa scale: 1mm on image = 400mm on chart;
Slit width = 5 microns

about 30% of the rejections. The largest single cause of rejection was the imperfections of the emulsions, either inherent or exemplified by "processing" pinholes. Particles of dust, dirt, glass, and similar materials occasionally adhered to the emulsion prior to or during exposure. Since their presence prevented exposure at that point, they became transparent holes after fixation. Pre-cleaning with air and brushing did not always alleviate this condition.

The major difficulty in the entire process is the centering of the mask over the center of rotation of the turntable. This is a trial and error problem, and its successful solution lies in the ability of the "centerer" to judge how much (and where) is to be filed off the mask aperture. Interpreting the test results for the next correction is an art.

There exists a physical limit on filter size and shape which is determined by the ability to cut out and file the aperture in the mask to the desired degree of precision. While this limit was not actually determined, it is felt that the practical limit for the Gaussian filters is reached for an $\underline{a}$ of 128. To obtain a feeling for this, refer to Figure 15b, which shows the mask corresponding to an $\underline{a}$ of 32. However, the Gaussian series could be extended beyond a = 128 if required, by making the filters in two photographic steps. This would then place the sensitive filing operation on the other end of the aperture which would make a negative of the desired filter in the first step. Since the image degrading characteristics of the first plate would carry over to the second (with its own problems of dust, dirt, non-uniformity) this method was not deemed sufficiently useful to warrant serious consideration in these investigations.

The filters which were made for installation in the Image Enhancement Viewer represent a set which was chosen to illustrate the filter shapes over the unmodified system passband, as detailled in the discussions of Section III leading to Table 3. The glass quality limits the usefulness of this set to the two smallest filter sizes (#3 and #4).

5.4 FILTER MATERIAL QUALITY

The glass on which the filters are held serves as the chief practical limitation of these filters. The unevenness of the emulsion and relative unflatness of the glass distorts the higher frequency content of the image and thereby destroys the fine detail. The fact that the information content out to 40 lines/mm is relatively distortion-free is remarkable, considering the 0.060 inch (nominal) thickness of the plates. Variation in distortion and focus for different areas of the same plate limit the usefulness of such filter material in a precision coherent optical system such as the Image Enhancement Viewer. In a system using heterochromatic illumination, such a slight focal shift might not be too bothersome. With monochromatic illumination, as in the Viewer, the shift is disastrous. The depth of focus is exquisitely narrow, and will not absorb even a minute change in image position, considering the spatial frequency range of interest. Finer focusing mechanisms must therefore be provided before these particular filters can be properly used.

5.5 THE PHOTOGRAPHIC PROCESS

While the photographic process, per se, appears adequate for use in such filters, the photographic plates (at least those commercially obtainable) are definitely not. The glass must be of sufficient quality so that it does not deform a plane wave passing through it. While flatness is essential for several reasons, the deformation is minimized by having the plate surfaces parallel. Since plates of this quality are not generally available, they must first be made and then coated with an emulsion.

The cost and time required for their manufacture are inversely proportional to the thickness. Plates 1/8 inch thick would cost about three times plates of 3/8 thickness. Glass plates whose surfaces have been parallel to within the required tolerance have been made in the Itek optical shop, in 0.050 thickness and 10 inches in diameter. Thus, a technological "breakthrough" is

not necessarily required, insofar as the plates are concerned. However, these laboratories do not presently possess the capability for the precisely thin emulsion manufacture and coating required for these filters. Research is presently being carried out in the Photographic Department which will lead to the required emulsion technology, but this does not lie in the near future. The cost of coating small lots (24 - 36 circular glass blanks) outside these laboratories is prohibitive, so that if research were continued on the photographic methods for fabricating filters a research and development study would be necessary to improve and extend the current coating technology.

The resulting thickness of such filters (conceivably as large as 0. 75 inch with lamination) would require special supporting structure and a definite modification of the Image Enhancement Viewer's filter wheels. Further, because of the quality of the glass required, there must be a minimal manufacturing rejection rate on the finished filters. Thus, the exposing equipment and techniques must be improved by a whole order of magnitude.

It may be concluded that filters made through the photographic process on available glass plates are not sufficiently free of image degrading characteristics to warrant further development. By bettering the glass and improving the techniques, it still might be possible to produce useful filters photographically, but it is felt that there are better and less devious ways to produce frequency attenuating filters.

From these studies also comes the conclusion that any glass which is placed in the optical system must be of at least quarter-wave flatness if the full image quality is to be achieved. The feeling also persists that the less glass in the system, the better, and that methods of filtering which use no supporting glass are preferred.

6. RECOMMENDATIONS

In view of the established feasibility of frequency attenuating filters, and the development of a basic technique of manufacture, several recommendations for future equipment development can easily be presented. However, the limitations of the methods and materials disclosed by these investigations call for a deeper inquiry into the ultimate usefulness and purpose of the Image Enhancement Viewer.

The occluding filters presently used on the Viewer serve a useful purpose in providing a definite mensurational capability. They cause no image deformation and the diffraction limit of the optical system is modified by their use in a known and controllable manner. Their continued use and installation in the Image Enhancement Viewer is definitely recommended.

Frequency attenuating filters serve a useful, demonstrable purpose in providing an enhancement capability for the Viewer. Were the filter material without image-deforming flaws, these filters could be used out to the system diffraction limit. As the test results have shown, the present Gaussian spatial filters destroy image quality in details in excess of 40 lines/mm, even though they provide the desired enhancement below this value. Thus, regions of fine detail which lie near the system frequency limit cannot be observed clearly in the image, let alone be enhanced. It is therefore recommended that the spatial filters developed for this program not be installed and used in the Image Enhancement Viewer except for photographic transparencies whose frequency content lies below 40 lines/mm.

An additional consideration which favors non-installation of these filters is the focal shift resulting from glass and emulsion thickness variations. To fully realize the information contained in the image, the focus must be constantly checked and adjusted. The Viewer does not presently have such a capability.

The demonstrated effects of such filters warrant further investigation, in both theoretical and practical aspects. The photographic method, by virtue of the relatively poor glass quality, is not suited for high-resolution linear imagery. It is therefore recommended that photographic methods using the commercially available glass plates of the quality used for these investigations be used in the future only for development and testing of new filter types. Based on the fabrication principles developed in this study it is further recommended that the means for producing practical, high-quality spatial filters be developed through the evaporative or mechanical methods if further studies in these areas indicate feasibility.

In view of the possibility of obtaining plates with the properly parallel surfaces and of developing an adequate emulsion technology, the photographic method should not be entirely dropped from serious consideration. Future studies should continually be measured against these possibilities since they represent a demonstrably feasible means for manufacturing frequency attenuating filters.

Because the effects of frequency attenuation are subtle, they must be viewed under suitable magnification. This naturally varies with the information content (and scale factor) of the transparency under study. Further, in order to realize the benefit of such filtering, photographic recording must be precise, with the focal plane determined accurately. The Image Enhancement Viewer cannot meet these two requirements without modification in the viewing plane of the system.

Therefore, it is recommended that should additional research be carried out with an end to equipping the Viewer with full-range frequency attenuating filters, it should be carried out in parallel with an engineering modification program. This program would provide a means for variable magnification of the image, more precise location of the focal plane, and a more versatile (70mm, Robot) photographic system at the image plane.

Finally, because a full understanding of the process is basic to further development, it is recommended that additional studies be made with regard to frequency attenuating filters, image enhancement, and optimum filtering. Such a program is necessary to extend the useful results reported here and exploit more fully the obvious advantages of image enhancement.

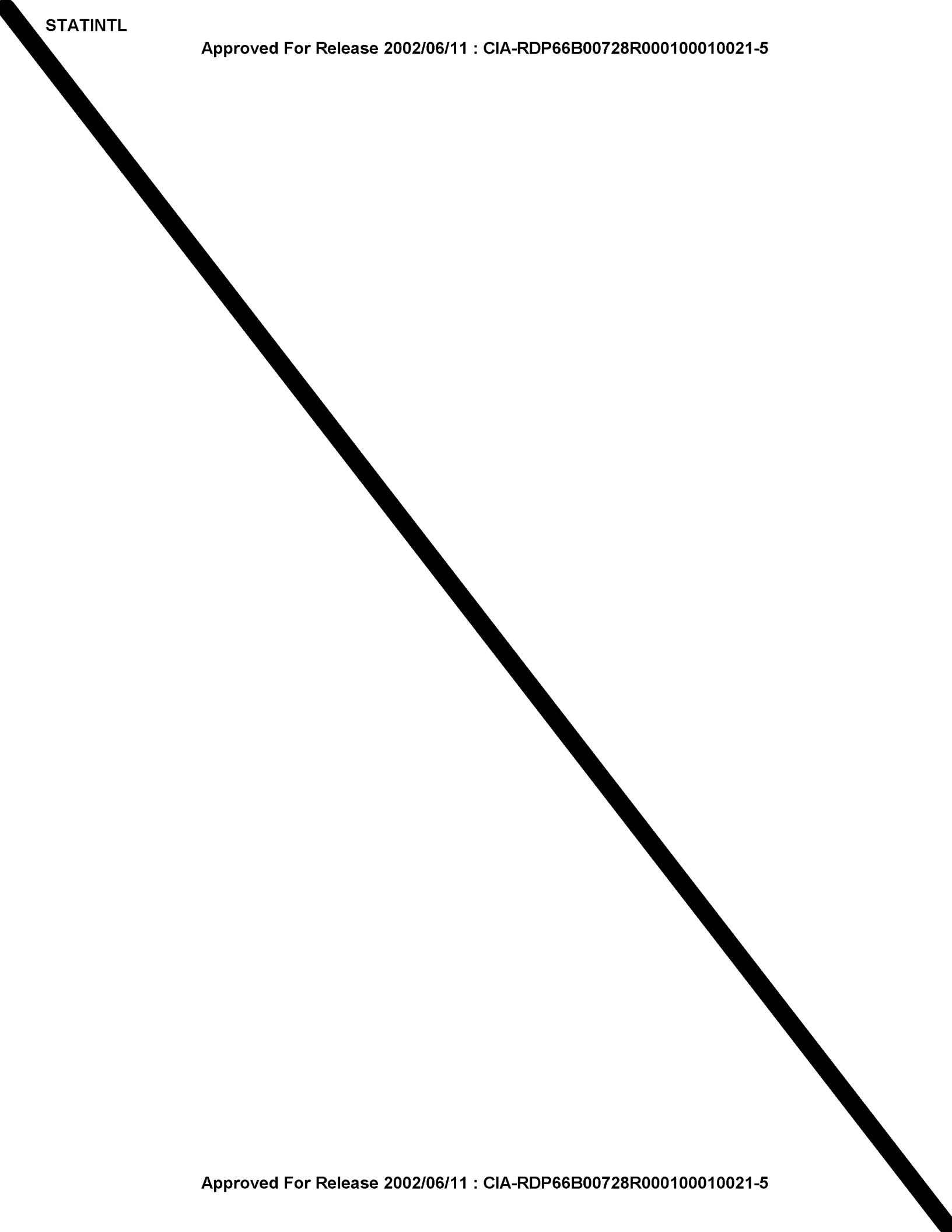

Approved For Release 2002/06/11 : CIA-RDP66B00728R000100010021-5